Electronic Supplementary Information

Oxidative coupling of 3-ethoxy Pd^{II} N-confused porphyrins with β-diketones using PIFA as the oxidant

Jieqing Huang, [a] Wenrui Yang, [a] Sijie Wen, [a] Zenan Zheng, [a] Xiaolin Chen, [a] Xiaofan Gan, [a] Ling Xu, [b] and Hua-Wei Jiang* [a]

a. School of Chemistry, South China Normal University, Guangzhou 510006, P. R. China E-mail: jiang@m.scnu.edu.cn.
b. Key Laboratory of Chemical Biology and Traditional Chinese Medicine Research, Ministry of Education, Key Laboratory of the Assembly and Application of Organic Functional Molecules of Hunan Province, College of Chemistry and Chemical Engineering, Hunan Normal University, Changsha 410081, China
* Corresponding authors.

Content

1. General Information

All chemicals that are commercially available were used without further purification unless otherwise noted. Thin-layer chromatography (TLC) was performed on silica gel plates (GF-254). Column chromatography was carried out by using silica gel (200−300 mesh). ^{1}H and ^{13}C NMR spectra were recorded on the Bruker AVANCE NEO 600 or JNM-ECZ500R/S1 spectrometer (operating as 600 MHz or 500 MHz for ^{1}H and 151 MHz or 126 MHz for ^{13}C) using the residual solvent as the internal reference for ^{1}H (δ = 7.26 ppm in $CDCl_3$) and ^{13}C (δ = 77.16 ppm in $CDCl_3$). UV-vis spectra studies were performed on a Shimadzu UV-2700 spectrophotometer.

2. Experimental Details and Characterization

Synthesis of **C-3 ethoxy Ag(III) NCP**

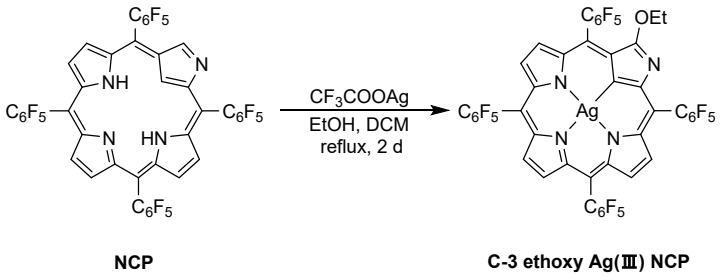

NCP C-3 ethoxy Ag(Ⅲ) NCP

Scheme S1. Synthesis of **C-3 ethoxy Ag(III) NCP**

To a solution of NCP (50 mg, 0.05 mmol) in CH_2Cl_2 (10 mL) were added the corresponding alcohol (2 mL) and CF_3COOAg (100 mg, 0.45 mmol). The mixture was stirred under reflux in air for 2 days. After cooling to room temperature, the reaction mixture was diluted with CH_2Cl_2 and washed with water. The organic layer was dried over anhydrous Na_2SO_4 and concentrated under reduced pressure. The crude product was purified by silica gel column chromatography to afford the **3-ethoxy Ag(III) NCP**.

C-3 ethoxy Ag(III) NCP: yield 75%. **^{1}H NMR** (600 MHz, $CDCl_3$): δ = 8.92 (d, *J* = 4.9 Hz, 1H, β-H), 8.88 (d, *J* = 4.9 Hz, 1H, β-H), 8.79 (t, *J* = 5.2 Hz, 3H, β-H), 8.72 (d, *J* = 4.9 Hz, 2H, β-H), 4.87 (q, *J* = 7.2 Hz, 2H, O$\underline{CH_2}CH_3$), 1.45 (t, *J* = 7.1 Hz, 3H, OCH$_2\underline{CH_3}$). **^{13}C NMR** (151 MHz, $CDCl_3$): δ = 171.06, 151.92, 147.44, 145.80, 142.81, 142.12, 140.80, 139.36, 139.01, 139.00, 138.66, 138.65, 138.29, 138.21, 137.59, 136.69, 130.88, 129.32, 129.14, 128.99, 128.30, 127.87, 116.66, 115.41, 110.83, 106.96, 105.52, 103.72, 65.47, 14.27. **MS (MALDI)** m/z: $[M+H]^+$ calcd for $C_{46}H_{12}ON_4AgF_{20}^+$ 1122.9737; found 1122.9707.

Synthesis of compound **C-3 ethoxy NCP**

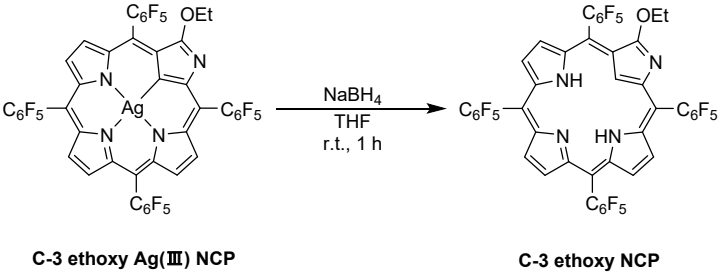

C-3 ethoxy Ag(Ⅲ) NCP C-3 ethoxy NCP

Scheme S2. Synthesis of **C-3 ethoxy NCP**

To a solution of **3-ethoxy Ag(III) NCP** (30 mg, 0.027 mmol) in THF (8 mL) was added a solution of $NaBH_4$ (71.2 mg, 1.88 mmol) in ethanol (6 mL). The resulting mixture was stirred at room temperature for 1 h. The reaction was then quenched by the addition of CH_2Cl_2 and washed with water. The organic layer was separated, dried over Na_2SO_4, and concentrated under reduced pressure. The residue was purified by silica gel column chromatography. The green fraction was collected and concentrated, and the product was recrystallized from CH_2Cl_2/n-hexane to afford violet crystals.

C-3 ethoxy NCP: yield 64%. **^{1}H NMR** (600 MHz, $CDCl_3$): δ = 8.81 (t, *J* = 4.8 Hz, 2H, β-H), 8.65 (d, *J* = 5.0 Hz, 1H, β-H), 8.61 (d, *J* = 4.8 Hz, 2H, β-H), 8.55 (d, *J* = 4.8 Hz, 1H, β-H), 4.69 (q, *J* = 7.2 Hz, 2H, O$\underline{CH_2}$$CH_3$), 1.35 (t, *J* = 7.1 Hz, 3H, $OCH_2\underline{CH_3}$), -2.52 (d, *J* = 106.6 Hz, 2H, inner-NH), -5.36 (s, 1H, 21C-H). **^{13}C NMR** (151 MHz, $CDCl_3$): δ = 169.99, 156.93, 154.75, 149.52, 139.30, 138.44, 137.13, 136.90, 134.84, 133.75, 128.14, 127.94, 126.45, 126.03, 124.91, 107.93, 105.55, 104.26, 103.32, 100.79, 66.09, 14.23. **MS (MALDI)** m/z: $[M+H]^+$ calcd for $C_{46}H_{15}ON_4F_{20}^+$ 1019.0921; found 1019.0883.

Synthesis of compound **Pd1**

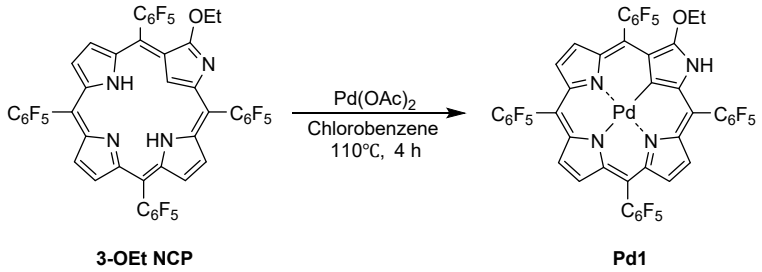

Scheme S3. Synthesis of **Pd1**

3-Ethoxy NCP (50 mg, 0.05 mmol) and $Pd(OAc)_2$ (33.7 mg, 0.15 mmol) were dissolved in chlorobenzene (20 mL). The mixture was stirred at 110 °C for 4 h. After removal of the solvent under reduced pressure, the residue was purified by flash column chromatography on silica gel. Recrystallization from CH_2Cl_2/n-hexane afforded **Pd1** as a purple-black solid.

Pd1: yield 51%. **^{1}H NMR** (600 MHz, $CDCl_3$): δ = 9.31 (s, 1H, outer-NH), 8.31 (d, *J* = 5.0 Hz, 1H, β-H), 8.23 (d, *J* = 4.9 Hz, 1H, β-H), 8.20 (d, *J* = 5.1 Hz, 1H, β-H), 8.18 (m, 3H, β-H), 4.80 (q, *J* = 7.0 Hz, 2H, O$\underline{CH_2}$$CH_3$), 1.54 (t, *J* = 7.0 Hz, 3H, $OCH_2\underline{CH_3}$). **^{13}C NMR** (151 MHz, $CDCl_3$): δ = 168.74, 147.76, 147.24, 144.25, 143.87, 142.73, 139.81, 132.80, 131.11, 130.37, 129.67, 128.38, 127.95, 127.44, 125.74, 112.14, 111.23, 106.91, 104.69, 101.86, 69.36, 14.00. **MS (MALDI)** m/z: $[M]^+$ calcd for $C_{46}H_{12}ON_4F_{20}Pd^+$ 1121.9721; found 1121.9722. **UV/Vis** (CH_2Cl_2): λ_{max} (lg ε) = 452 (4.84), 535 (3.89), 573 (3.87), 620 (3.72) and 668 nm (3.92).

Synthesis of compound **Pd1a**

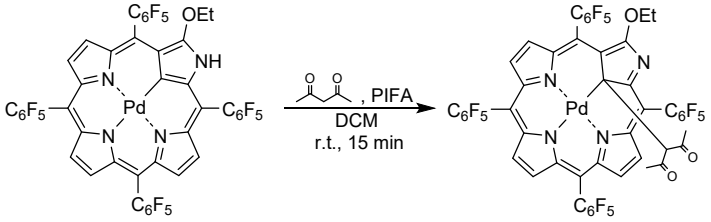

Pd1 **Pd1a**

Scheme S4. Synthesis of **Pd1a**

Pd1 (30 mg, 0.027 mmol), PIFA (17.4 mg, 0.04 mmol) and acetylacetone (0.06 mL) were combined in CH_2Cl_2 (10 mL). The mixture was stirred at room temperature for 15 min, then diluted with additional CH_2Cl_2 and washed with saturated aqueous NaCl solution. The organic layer was dried over anhydrous Na_2SO_4 and concentrated under reduced pressure. The residue was purified by flash column chromatography on silica gel to afford **Pd1a**.

Pd1a: yield 73%. **^{1}H NMR** (600 MHz, $CDCl_3$): δ = 8.41 (d, *J* = 5.0 Hz, 1H, β-H), 8.37 (m, 2H, β-H), 8.34 (d, *J* = 4.0 Hz, 1H, β-H), 8.33 (d, *J* = 4.8 Hz, 1H, β-H), 8.27 (d, *J* = 4.6 Hz, 1H, β-H), 5.05 (m, 1H, O$\underline{CH_2}$CH$_3$), 4.61 (m, 1H, O$\underline{CH_2}$CH$_3$), 1.37 (t, *J* = 7.1 Hz, 3H, OCH$_2\underline{CH_3}$), 0.59 (s, 3H, CH(CO$\underline{CH_3}$)$_2$), -0.29 (s, 3H, CH(CO$\underline{CH_3}$)$_2$), -0.57 (s, 1H, $\underline{CH}$(COCH$_3$)$_2$). **^{13}C NMR** (151 MHz, $CDCl_3$): δ = 194.74, 194.69, 180.56, 172.76, 155.89, 152.24, 145.13, 144.46, 142.76, 142.66, 139.10, 135.55, 133.48, 131.07, 130.88, 130.14, 129.07, 117.56, 114.07, 109.82, 69.23, 67.87, 43.64, 28.91, 28.73, 14.21. **MS (MALDI)** m/z: $[M]^+$ calcd for $C_{51}H_{18}O_3N_4F_{20}Pd^+$ 1220.0089; found 1220.0098. **UV/Vis** (CH_2Cl_2): λ_{max} (lg ε) = 358 (4.50), 424 (4.54), 465 (4.50), 514 (4.22) and 681 nm (4.31).

Synthesis of compound **Pd1b**

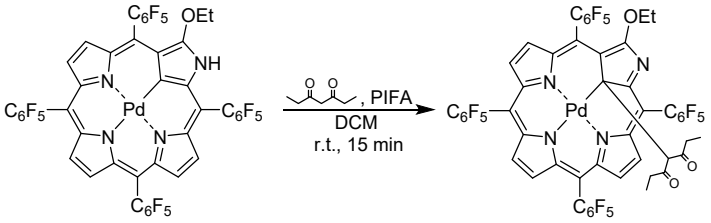

Pd1 **Pd1b**

Scheme S5. Synthesis of **Pd1b**

Pd1 (30 mg, 0.027 mmol), PIFA (17.4 mg, 0.04 mmol) and 3,5-heptanedione (0.08 mL) were combined in CH_2Cl_2 (10 mL). The mixture was stirred at room temperature for 15 min, then diluted with additional CH_2Cl_2 and washed with saturated aqueous NaCl solution. The organic layer was dried over anhydrous Na_2SO_4 and concentrated under reduced pressure. The residue was purified by flash column chromatography on silica gel to afford **Pd1b**.

Pd1b: yield 66%. **^{1}H NMR** (600 MHz, $CDCl_3$): δ = 8.41 (d, *J* = 5.0 Hz, 1H, β-H), 8.36 (m, 3H, β-H), 8.31 (d, *J* = 4.7 Hz, 1H, β-H), 8.27 (d, *J* = 4.7 Hz, 1H, β-H), 5.01 (m, 1H, O$\underline{CH_2}$CH$_3$), 4.58 (m, 1H, O$\underline{CH_2}$CH$_3$), 1.33 (t, *J* = 7.4 Hz, 3H, OCH$_2\underline{CH_3}$), 0.75 (m, 1H, CH(CO$\underline{CH_2}$CH$_3$)$_2$), 0.64 (m, 1H, CH(CO$\underline{CH_2}$CH$_3$)$_2$), 0.19 (m, 1H, CH(CO$\underline{CH_2}$CH$_3$)$_2$), 0.15 (t, *J* = 7.1 Hz, 3H, CH(COCH$_2\underline{CH_3}$)$_2$), -

0.22 (m, 1H, CH(CO$\underline{CH_2}CH_3)_2$), -0.61 (s, 1H, $\underline{CH}(COCH_2CH_3)_2$), -0.81 (t, *J* = 6.8 Hz, 3H, $CH(COCH_2\underline{CH_3})_2$). **^{13}C NMR** (151 MHz, $CDCl_3$): δ = 197.01, 180.88, 172.58, 155.82, 152.37, 146.85, 145.05, 144.31, 142.93, 142.59, 139.79, 135.40, 133.13, 130.93, 130.70, 130.00, 129.09, 117.77, 114.07, 109.75, 67.83, 67.80, 43.79, 35.58, 35.10, 29.85, 14.18, 6.74, 5.58. **MS (MALDI)** m/z: $[M]^+$ calcd for $C_{53}H_{23}O_3N_4F_{20}Pd^+$ 1249.0480; found 1249.0470. **UV/Vis** (CH_2Cl_2): λ_{max} (lg ε) = 358 (4.47), 427 (4.53), 465 (4.48), 513 (4.19) and 681 nm (4.29).

Synthesis of compound **Pd2**

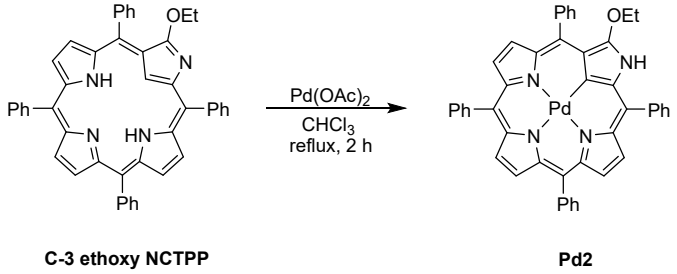

C-3 ethoxy NCTPP **Pd2**

Scheme S6. Synthesis of **Pd2**

C-3-Ethoxy NCTPP (100 mg, 0.15 mmol) and $Pd(OAc)_2$ (101.0 mg, 0.45 mmol) were combined in chloroform (15 mL). The mixture was stirred at 60 °C for 2 h. After removal of the solvent under reduced pressure, the residue was purified by flash column chromatography on silica gel. Recrystallization from CH_2Cl_2/n-hexane afforded **Pd2** as a purple-black solid.

Pd2: yield 46%. **^{1}H NMR** (600 MHz, $CDCl_3$): δ = 9.32 (s, 1H, β-H), 8.22 (d, *J* = 4.8 Hz, 1H, β-H), 8.19 (m, 3H, β-H), 8.16 (d, *J* = 4.9 Hz, 1H, β-H), 8.13 (d, *J* = 4.8 Hz, 1H, β-H), 8.04-7.97 (m, 6H, Ar–H), 7.79 (d, *J* = 6.5 Hz, 2H, Ar–H), 7.69-7.53 (m, 12H, Ar–H), 4.31 (q, *J* = 6.9 Hz, 2H, $O\underline{CH_2}CH_3$), 1.15(t, *J* = 6.9 Hz, 3H, $OCH_2\underline{CH_3}$). **^{13}C NMR** (151 MHz, $CDCl_3$): δ = 167.78, 147.36, 146.31, 144.48, 143.49, 142.91, 142.87, 142.56, 141.42, 139.87, 138.99, 133.90, 133.82, 132.85, 132.33, 131.69, 130.69, 130.20, 129.31, 129.19, 128.30, 128.03, 128.01, 127.69, 127.19, 126.84, 126.81, 126.72, 125.77, 124.57, 122.91, 120.72, 118.55, 111.88, 67.46, 13.79. **MS (MALDI)** m/z: $[M]^+$ calcd for $C_{46}H_{32}N_4OPd^+$ 762.1622; found 762.1550. **UV/Vis** (CH_2Cl_2): λ_{max} (lg ε) = 451 (5.02), 528 (3.97), 570 (3.60), 619 (3.78) and 667 nm (4.06).

Synthesis of compound **Pd2a**

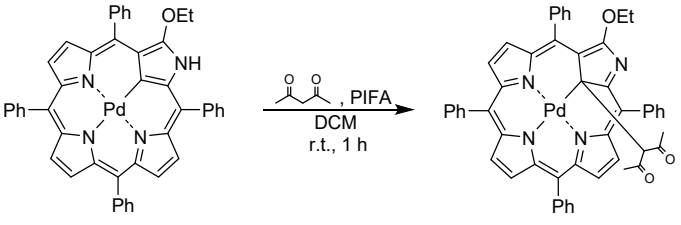

Pd2 **Pd2a**

Scheme S7. Synthesis of **Pd2a**

Pd2 (50 mg, 0.07 mmol), PIFA (42.3 mg, 0.10 mmol) and acetylacetone (0.05 mL) were combined in CH_2Cl_2 (7 mL). The mixture was stirred at room temperature for 1 h, then diluted with additional CH_2Cl_2 and washed with saturated aqueous NaCl solution. The organic layer was

dried over anhydrous Na_2SO_4 and concentrated under reduced pressure. The residue was purified by flash column chromatography on silica gel to afford **Pd2a**.

Pd2a: yield 62%. **^{1}H NMR** (600 MHz, $CDCl_3$): δ = 8.68 (s, 1H, Ar–H), 8.50 (d, *J* = 4.9 Hz, 1H, β-H), 8.46 (d, *J* = 4.9 Hz, 1H, β-H), 8.41 (d, *J* = 4.8 Hz, 1H, β-H), 8.37 (d, *J* = 4.7 Hz, 1H, β-H), 8.30 (d, *J* = 4.6 Hz, 1H, β-H), 8.27 (d, *J* = 4.6 Hz, 1H, β-H), 8.15 (m, 2H, Ar–H), 8.09 (d, *J* = 6.7 Hz, 1H, Ar–H), 7.97 (d, *J* = 7.4 Hz, 1H, Ar–H), 7.76-7.61 (m, 15H, Ar–H), 4.81 (m, 1H, OCH_2CH_3), 4.10 (m, 1H, OCH_2CH_3), 1.09 (t, *J* = 7.0 Hz, 3H, OCH_2CH_3), 0.72 (s, 3H, $CH(COCH_3)_2$), -0.34 (s, 3H, $CH(COCH_3)_2$), -0.71 (s, 1H, $CH(COCH_3)_2$). **^{13}C NMR** (151 MHz, $CDCl_3$): δ = 197.01, 196.94, 176.92, 171.17, 155.37, 152.55, 145.37, 145.26, 144.05, 143.69, 141.52, 141.44, 141.18, 140.77, 136.15, 135.71, 134.94, 134.41, 134.33, 134.15, 133.76, 133.47, 132.94, 131.50, 130.53, 130.47, 130.32, 129.52, 128.23, 128.14, 128.11, 127.72, 127.50, 127.08, 126.94, 126.87, 126.14, 124.29, 77.37, 77.16, 76.95, 69.77, 65.98, 42.86, 29.96, 29.11, 14.22. **MS (MALDI)** m/z: $[M+H]^+$ calcd for $C_{51}H_{39}O_3N_4Pd^+$ 861.2052; found 861.2065. **UV/Vis** (CH_2Cl_2): λ_{max} (lg ε) = 363 (4.44), 421 (4.44), 477 (4.61), 502 (4.39) and 685 nm (3.98).

Synthesis of compound **Pd2b**

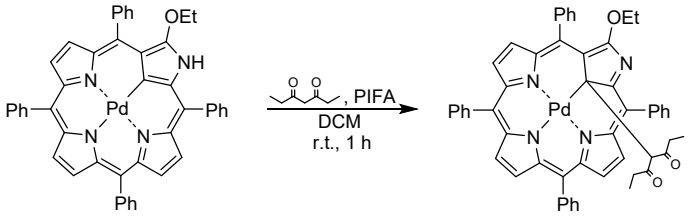

Scheme S8. Synthesis of **Pd2b**

Pd2 (50 mg, 0.07 mmol), PIFA (42.3 mg, 0.10 mmol) and 3,5-heptanedione (0.07 mL) were combined in CH_2Cl_2 (7 mL). The mixture was stirred at room temperature for 1 h, then diluted with additional CH_2Cl_2 and washed with saturated aqueous NaCl solution. The organic layer was dried over anhydrous Na_2SO_4 and concentrated under reduced pressure. The residue was purified by flash column chromatography on silica gel to afford **Pd2b**.

Pd2b: yield 60%. **^{1}H NMR** (500 MHz, $CDCl_3$): δ = 8.79 (s, 1H, Ar–H), 8.53 (d, *J* = 5.0 Hz, 1H, β-H), 8.48 (d, *J* = 5.0 Hz, 1H, β-H), 8.45 (d, *J* = 4.8 Hz, 1H, β-H), 8.35 (d, *J* = 4.8 Hz, 1H, β-H), 8.30 (d, *J* = 4.6 Hz, 1H, β-H), 8.28 (d, *J* = 4.6 Hz, 1H, β-H), 8.16 (d, *J* = 6.5 Hz, 1H, Ar–H), 8.10 (d, *J* = 7.1 Hz, 2H, Ar–H), 7.99 (d, *J* = 7.4 Hz, 1H, Ar–H), 7.80-7.60 (m, 15H, Ar–H), 4.80 (m, 1H, OCH_2CH_3), 4.08 (m, 1H, OCH_2CH_3), 1.05 (t, *J* = 7.1 Hz, 3H, OCH_2CH_3), 0.92 (m, 1H, $CH(COCH_2CH_3)_2$), 0.81 (m, 1H, $CH(COCH_2CH_3)_2$), 0.32 (t, *J* = 7.1 Hz, 3H, $CH(COCH_2CH_3)_2$), -0.03 (m, 1H, $CH(COCH_2CH_3)_2$), -.033 (m, 1H, $CH(COCH_2CH_3)_2$), -0.73 (s, 1H, $CH(COCH_2CH_3)_2$), -0.87 (t, *J* = 7.1 Hz, 3H, $CH(COCH_2CH_3)_2$). **^{13}C NMR** (126 MHz, $CDCl_3$): δ = 198.58, 198.21, 177.32, 171.09, 154.97, 152.61, 145.29, 145.03, 144.09, 143.57, 141.56, 141.48, 141.21, 140.70, 136.29, 134.73, 134.29, 133.87, 133.68, 133.31, 132.61, 131.28, 130.37, 130.32, 130.02, 129.53, 128.14, 128.07, 128.00, 127.69, 127.42, 127.04, 126.87, 126.80, 125.94, 123.95, 67.67, 65.87, 42.97, 36.20, 35.48, 31.68, 22.75, 14.11, 7.17, 5.77. **MS (MALDI)** m/z: $[M+H]^+$ calcd for $C_{53}H_{43}O_3N_4Pd^+$ 889.2365; found 889.2379. **UV/Vis** (CH_2Cl_2): λ_{max} (lg ε) = 363 (4.44), 422 (4.39), 477 (4.62), 502 (4.40) and 685 nm (4.00).

3. X-ray diffraction study

The single crystals of **Pd1** were obtained by vapor diffusion of n-hexane into its $CHCl_3$ solution at room temperature. Single-crystal X-ray diffraction analysis data were collected at 172 K with a Bruker APEX-II CCD diffractometer by using graphite monochromatic Mo-Kα radiation (λ = 0.71073 Å). The structures were solved by direct methods using ShelXS and refined using a full-matrix least-squares technique based on F^2 within ShelXL 2018 and OLEX-2.[25] Crystal data are compiled in Table S1.

The single crystals of **Pd2** were obtained by vapor diffusion of butanol into its $CHCl_3$ solution at room temperature. Single-crystal X-ray diffraction analysis data were collected at 150 K with a Bruker APEX-II CCD diffractometer by using graphite monochromatic Cu-Kα radiation (λ = 1.54178 Å). The structures were solved by direct methods using ShelXS and refined using a full-matrix least-squares technique based on F^2 within ShelXL 2018 and OLEX-2. Crystal data are compiled in Table S1.

Table S1. Crystal data and structure refinement for **Pd1a** and **Pd2a**.

	Compound **Pd1a**	Compound **Pd2a**
CCDC [a]	2529281	2529282
Empirical formula	$C_{55}H_{24}F_{20}N_4O_3Pd$	$C_{103}H_{77}Cl_3N_8O_6Pd_2$
Formula weight	1275.18	1841.87
Temperature/K	150.00	240.15
Crystal system	triclinic	triclinic
Space group	P-1	P-1
a/Å	13.0937(6)	10.478(2)
b/Å	13.6141(6)	14.544(3)
c/Å	15.2325(7)	14.623(3)
α/°	105.165(2)	80.817(15)
β/°	106.252(2)	73.450(17)
γ/°	93.443(3)	83.659(17)
Volume/Å^3	2489.9(2)	2103.8(8)
Z	2	1
ρ_{calc}g/cm^3	1.701	1.454
μ/mm^{-1}	4.155	4.831
F(000)	1264.0	942.0
Crystal size/mm^3	0.12 × 0.11 × 0.08	0.15 × 0.11 × 0.1
Radiation	Cu Kα (λ = 1.54178)	Cu Kα (λ = 1.54178)
2Θ range for data collection/°	6.798 to 133.186	6.17 to 117.86

Index ranges	$-15 \le h \le 15, -16 \le k \le 16, -18 \le l \le 18$	$-10 \le h \le 11, -16 \le k \le 16, -14 \le l \le 16$
Reflections collected	33593	15131
Independent reflections	8713 [R_{int} = 0.0687, R_{sigma} = 0.0608]	5806 [R_{int} = 0.0874, R_{sigma} = 0.0950]
Data/restraints/parameters	8713/0/753	5806/33/571
Goodness-of-fit on F^2	1.118	1.151
Final R indexes [I>=2σ (I)]	R_1 = 0.0729, Wr_2 = 0.2110	R_1 = 0.0934, Wr_2 = 0.2381
Final R indexes [all data]	R_1 = 0.0772, Wr_2 = 0.2173	R_1 = 0.1612, Wr_2 = 0.3161
Largest diff. peak/hole / e $Å^{-3}$	2.07/-1.70	1.07/-2.63

a: CCDC 2529281 and 2529282 contains the supplementary crystallographic data for this paper. These data can be obtained free of charge via www.ccdc.cam.ac.uk/data_request/cif, or by emailing data_request@ccdc.cam.ac.uk, or by contacting The Cambridge Crystallographic Data Centre, 12 Union Road, Cambridge CB2 1EZ, UK; fax: +44 1223 336033.

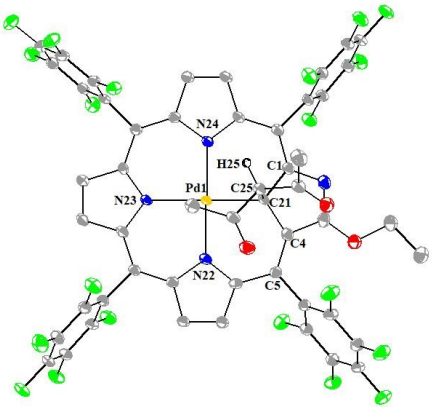

top view

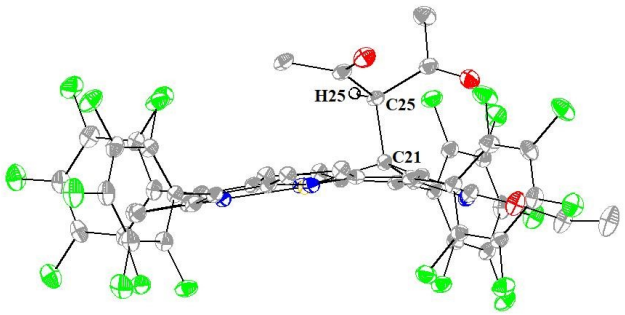

side view

Figure S1. X-ray crystal structure of **Pd1a**. Solvent molecules and all hydrogen atoms except for H25 are omitted for clarity.

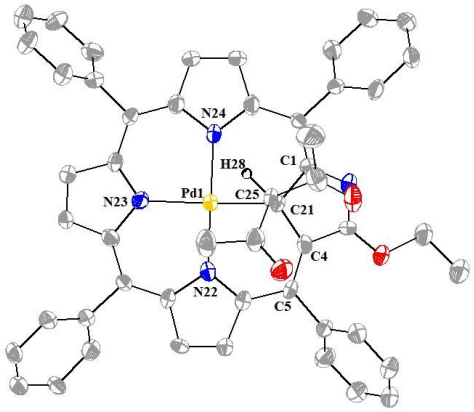

top view

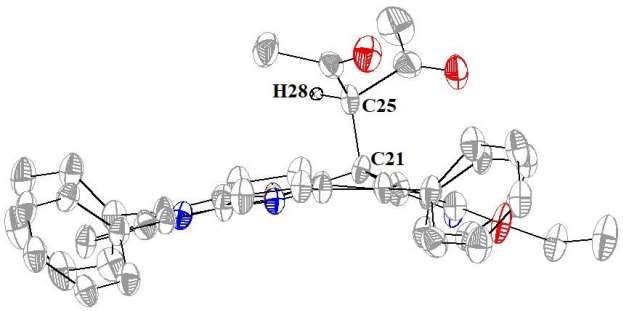

side view

Figure S2. X-ray crystal structure of **Pd2a**. Solvent molecules and all hydrogen atoms except for H28 are omitted for clarity.

4. UV/Vis Absorption Spectra

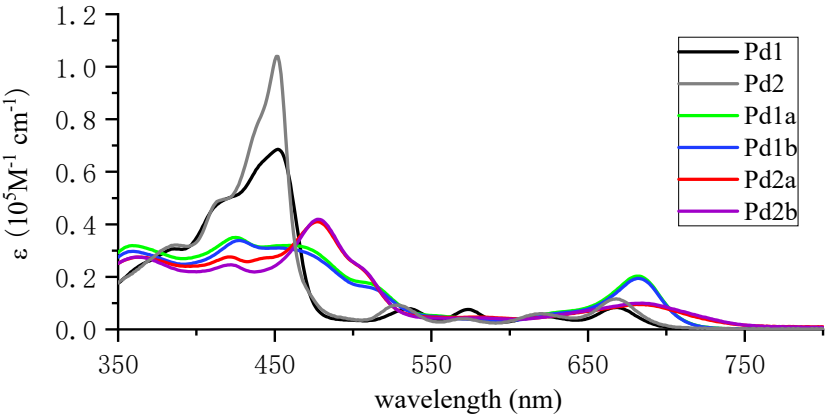

Figure S3. UV-vis absorption spectra of Compound **Pd1**, **Pd2**, **Pd1a-b**, and **Pd2a-b** in CH_2Cl_2.

5. NMR spectra

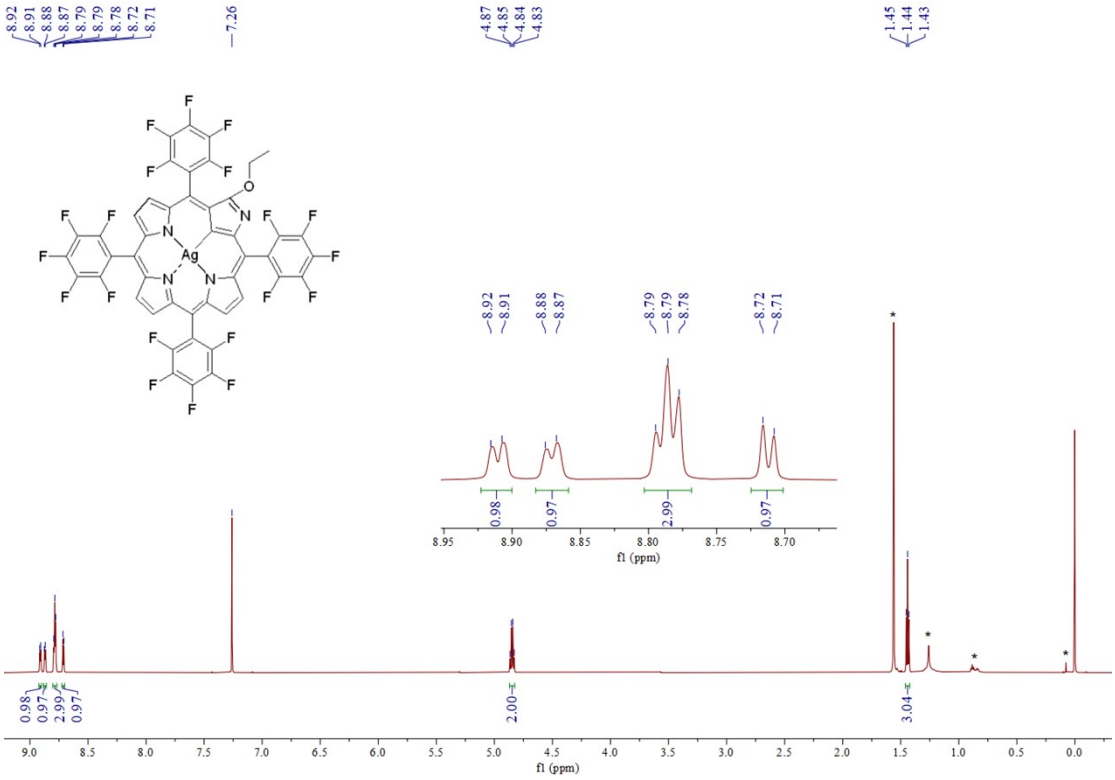

Figure S4. ^{1}H NMR (600 MHz, $CDCl_3$) spectrum of **C-3 ethoxy Ag(III) NCP**. [*] solvent impurities

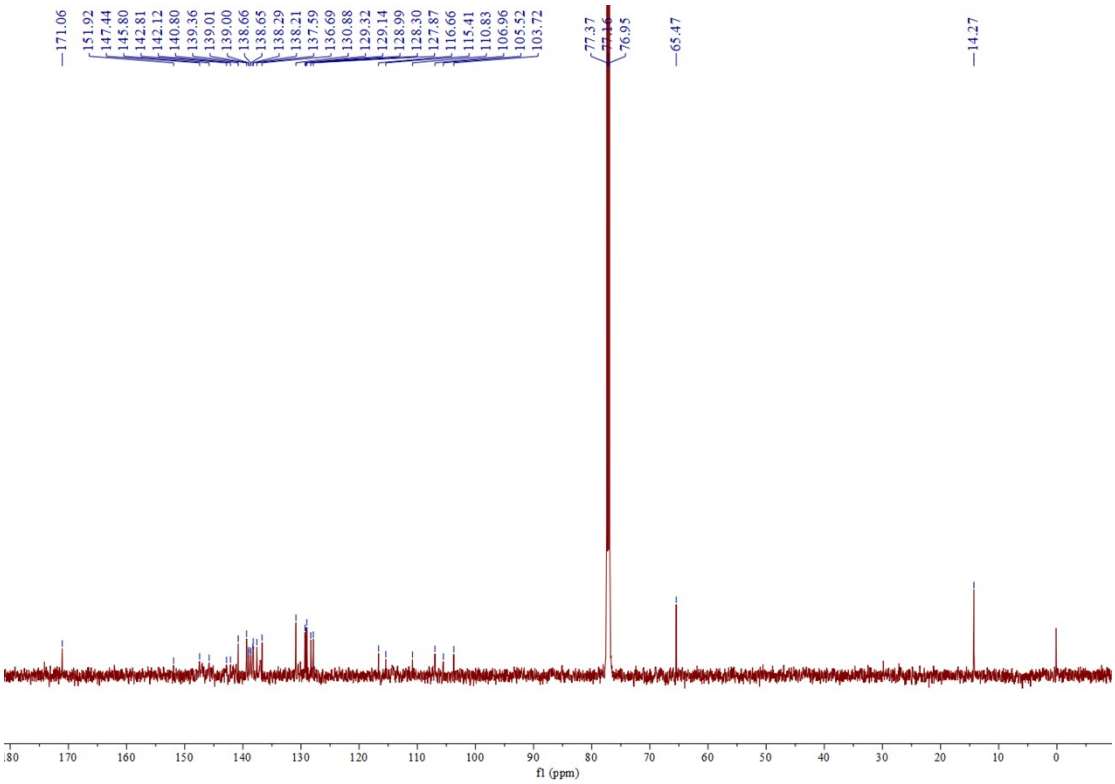

Figure S5. ^{13}C NMR (151 MHz, $CDCl_3$) spectrum of **C-3 ethoxy Ag(III) NCP**. [*] solvent impurities

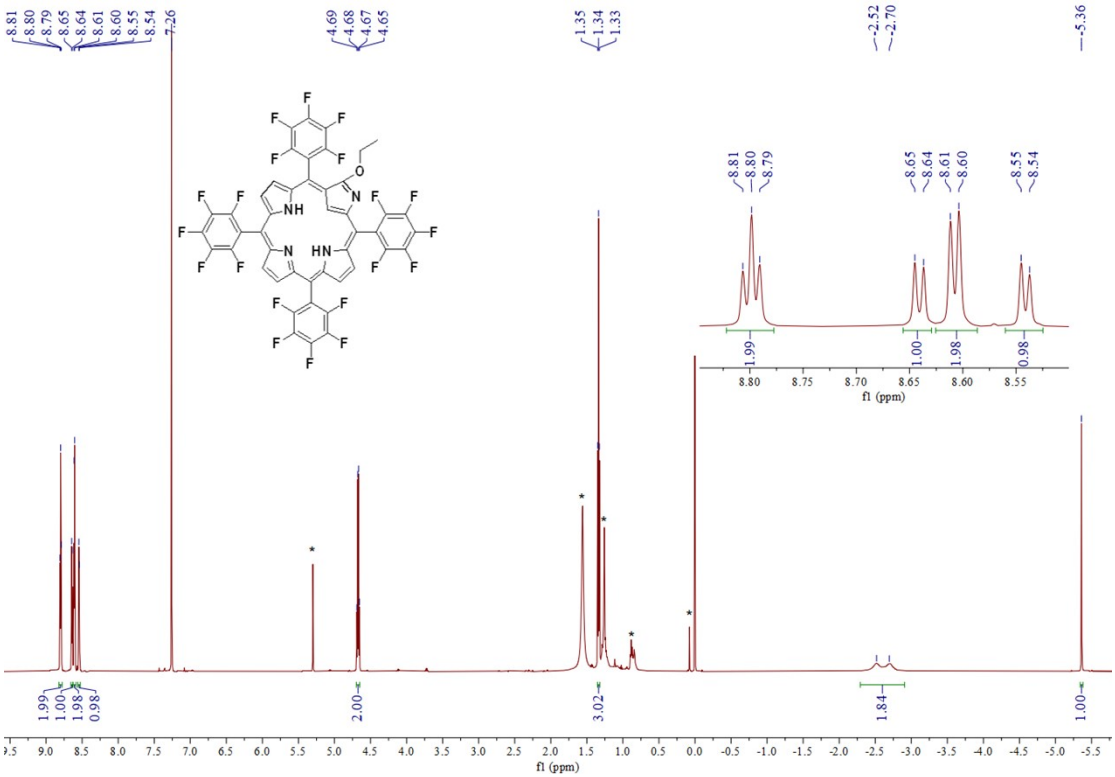

Figure S6. ^{1}H NMR (600 MHz, $CDCl_3$) spectrum of **C-3 ethoxy NCP**. [*] solvent impurities

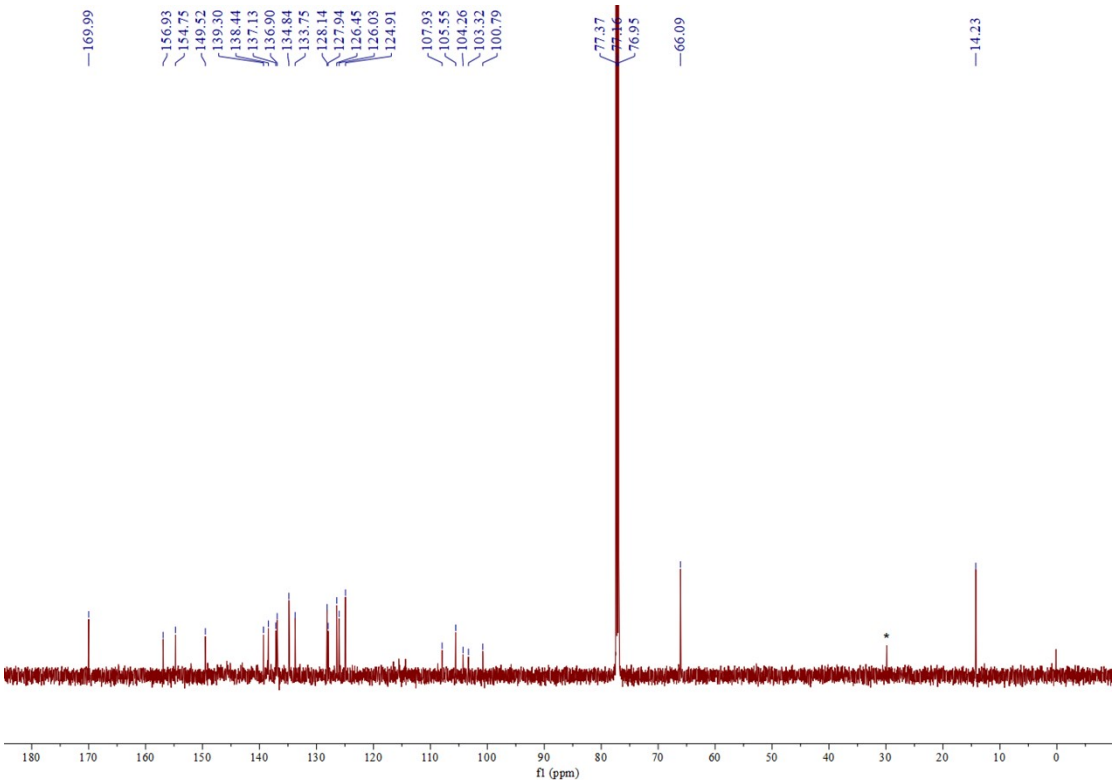

Figure S7. ^{13}C NMR (151 MHz, $CDCl_3$) spectrum of **C-3 ethoxy NCP**. [*] solvent impurities

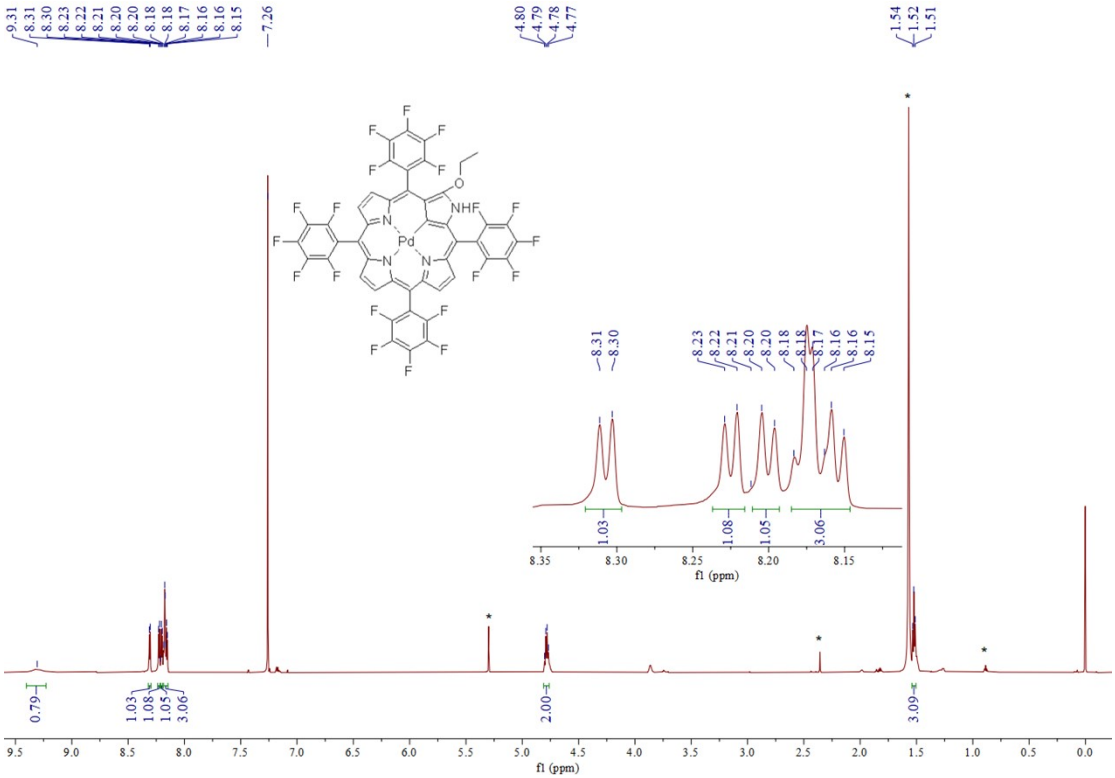

Figure S8. ^{1}H NMR (600 MHz, $CDCl_3$) spectrum of **Pd1**. [*] solvent impurities

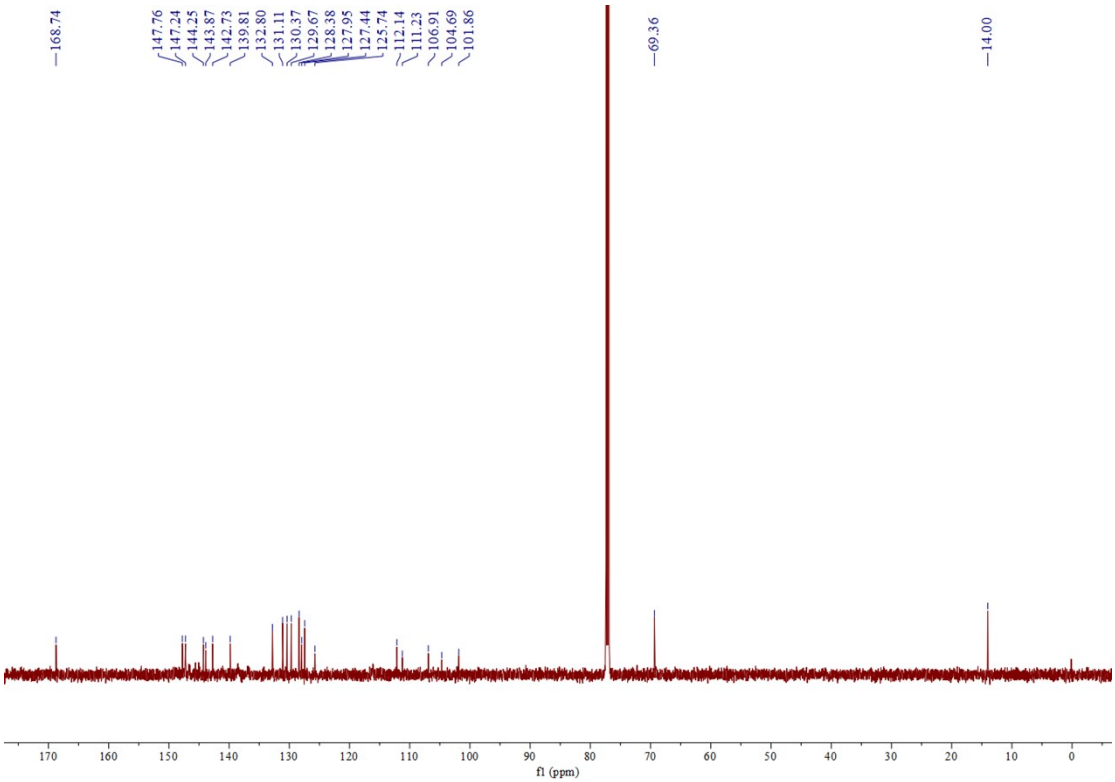

Figure S9. ^{13}C NMR (151 MHz, $CDCl_3$) spectrum of **Pd1**. [*] solvent impurities

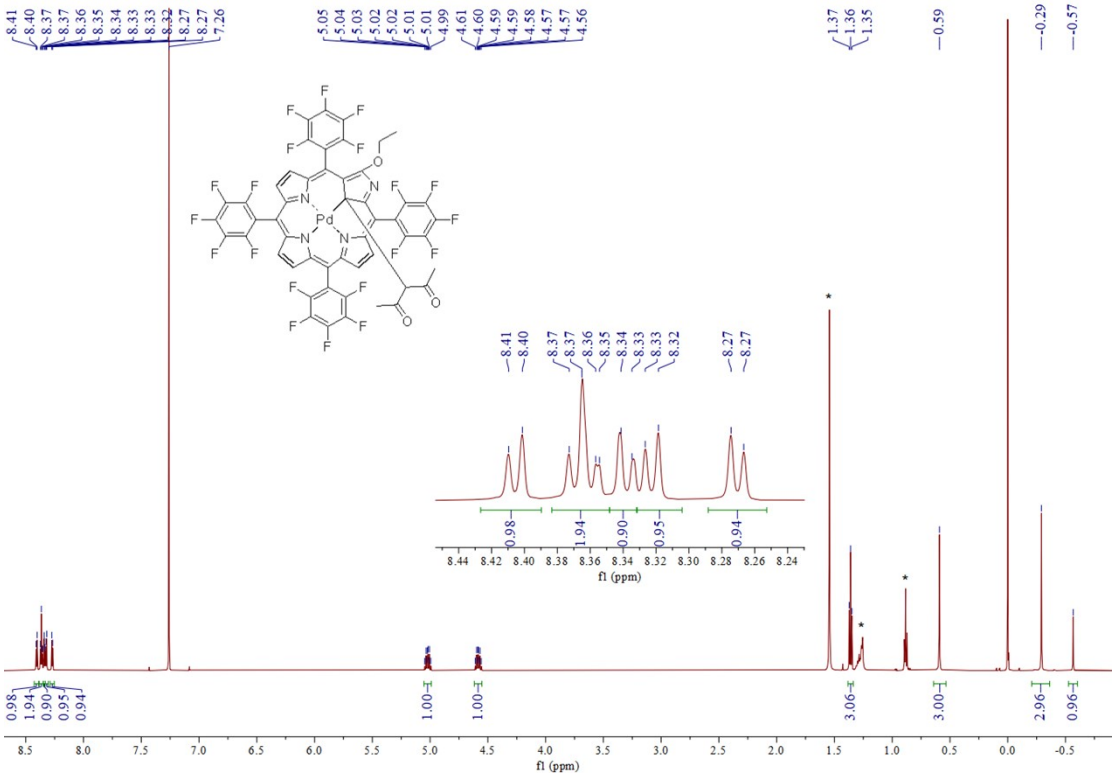

Figure S10. ^{1}H NMR (600 MHz, $CDCl_3$) spectrum of **Pd1a**. [*] solvent impurities

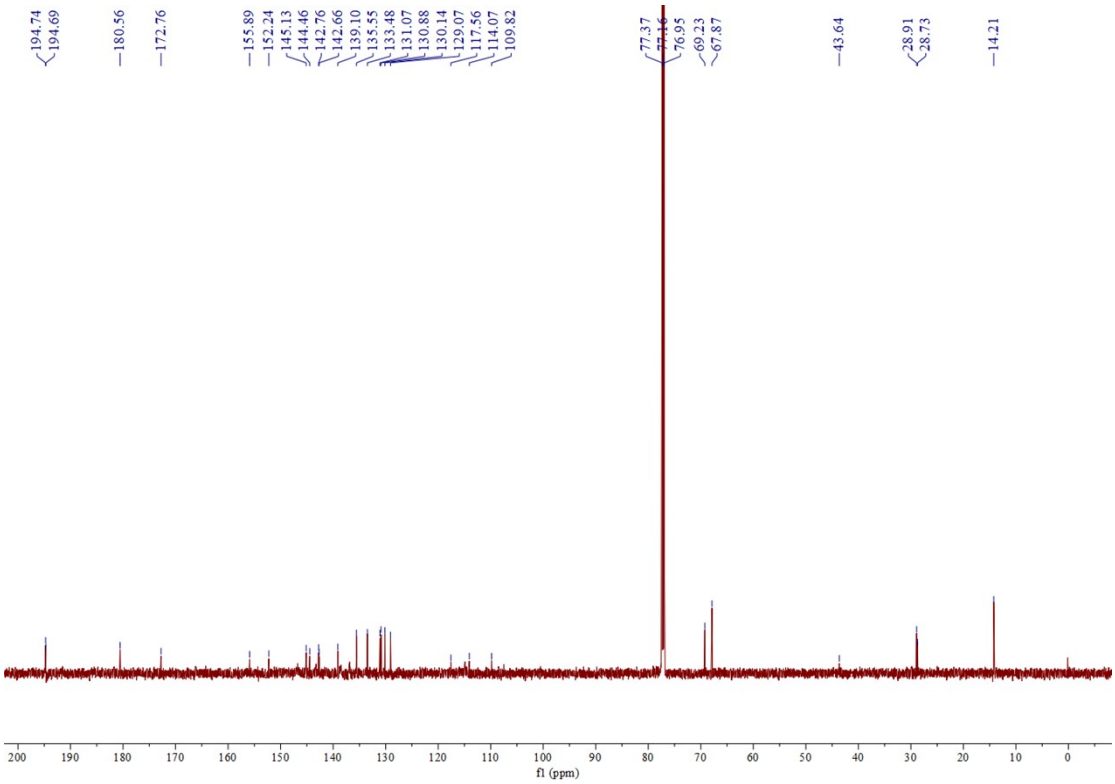

Figure S11. ^{13}C NMR (151 MHz, $CDCl_3$) spectrum of **Pd1a**.

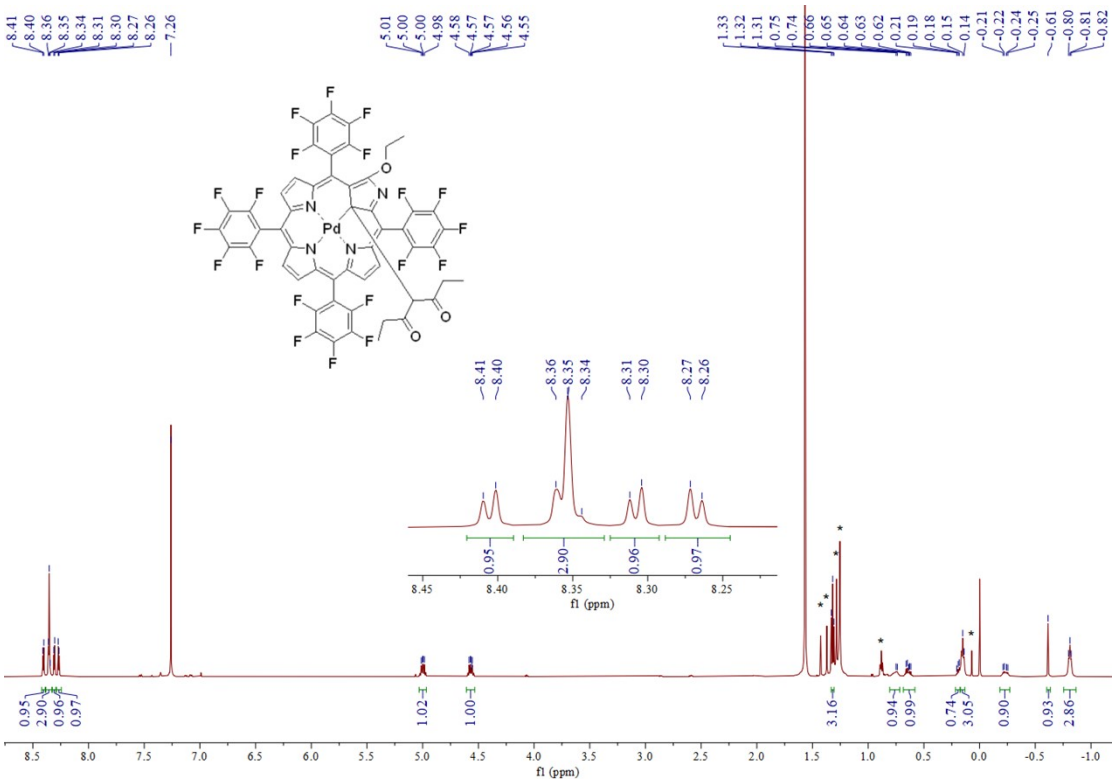

Figure S12. ^{1}H NMR (600 MHz, $CDCl_3$) spectrum of **Pd1b**. [*] solvent impurities

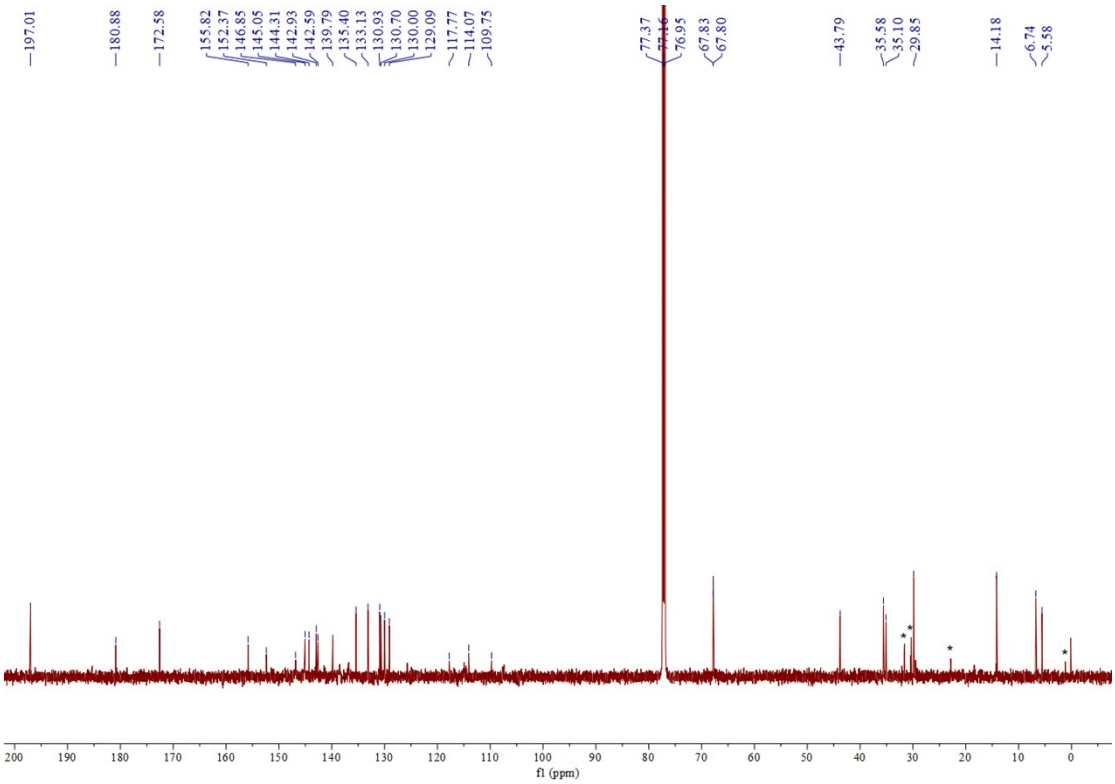

Figure S13. ^{13}C NMR (151 MHz, $CDCl_3$) spectrum of **Pd1b**. [*] solvent impurities

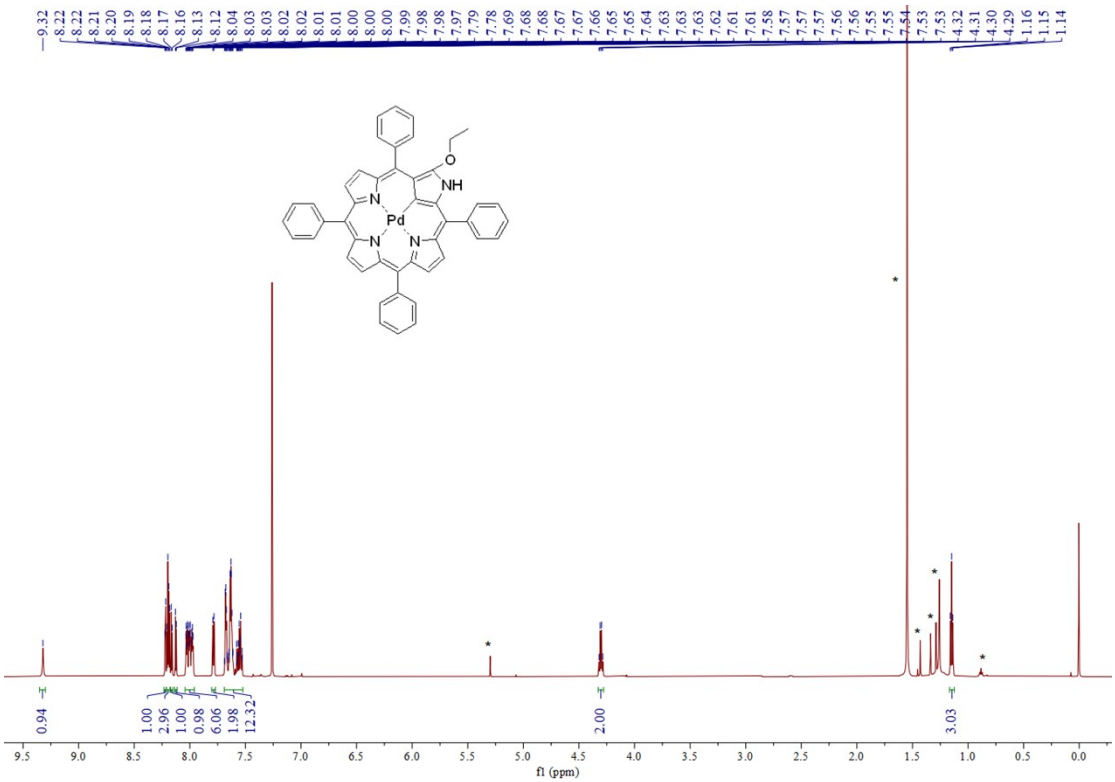

Figure S14. ^{1}H NMR (600 MHz, $CDCl_3$) spectrum of **Pd2**. [*] solvent impurities

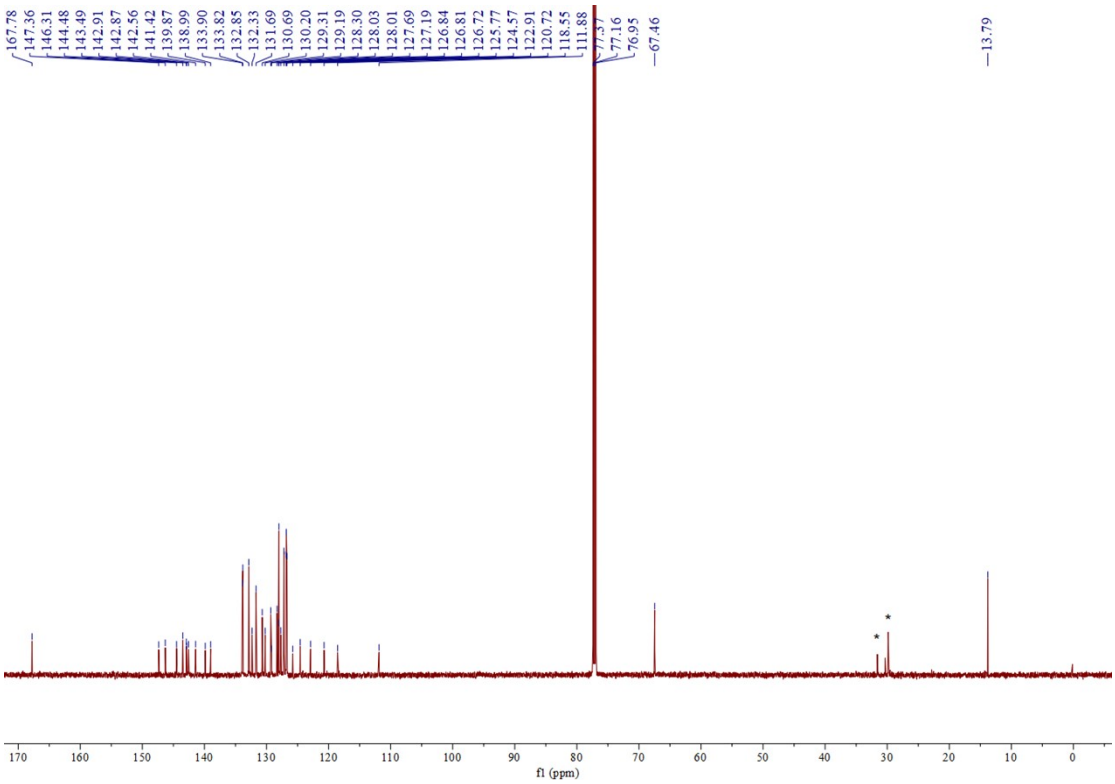

Figure S15. ^{13}C NMR (151 MHz, $CDCl_3$) spectrum of **Pd2**. [*] solvent impurities

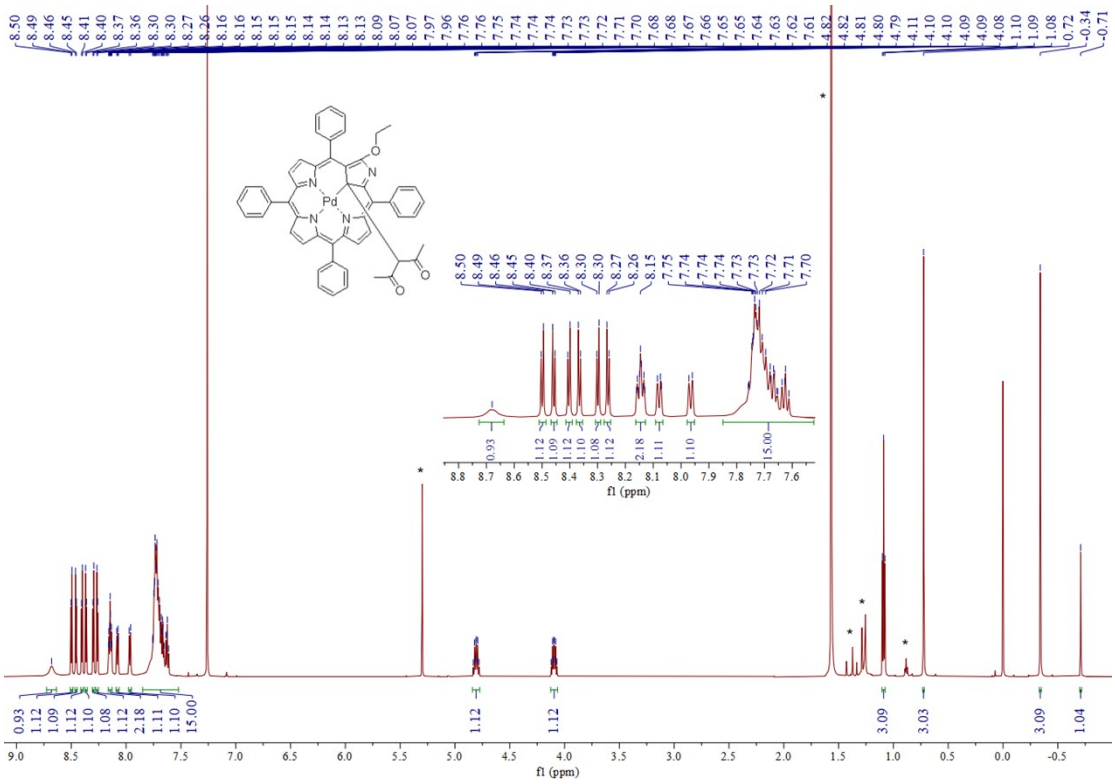

Figure S16. ^{1}H NMR (600 MHz, $CDCl_3$) spectrum of **Pd2a**. [*] solvent impurities

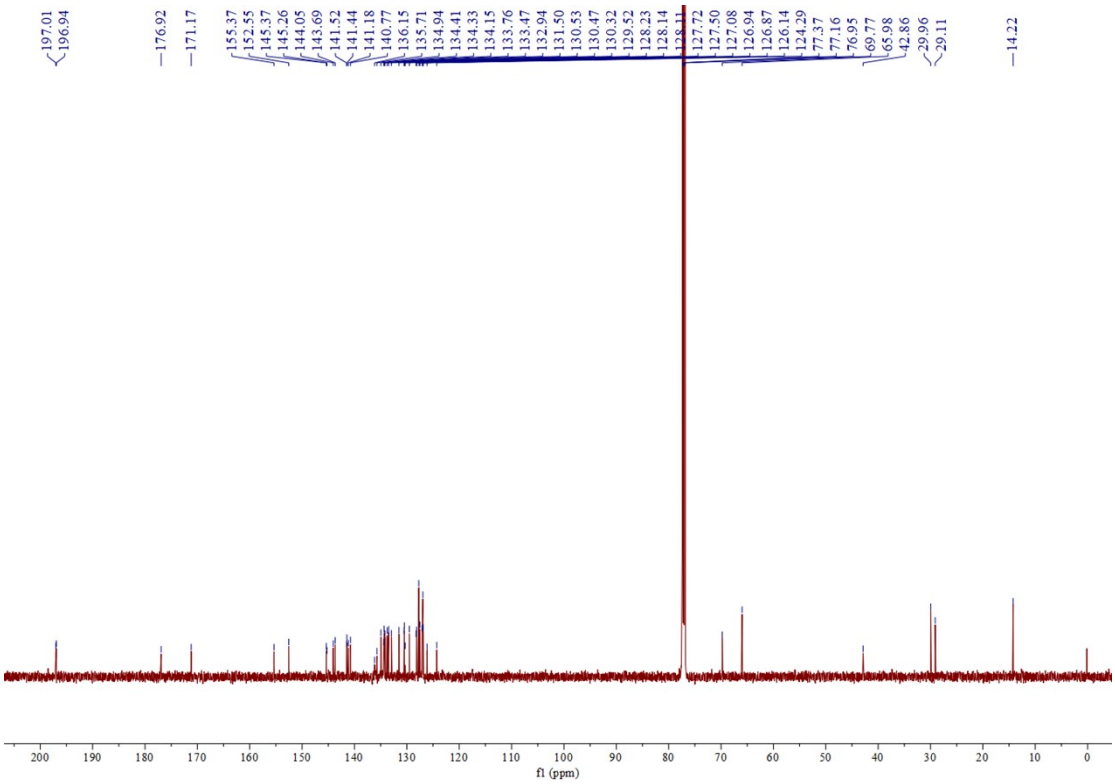

Figure S17. ^{13}C NMR (151 MHz, $CDCl_3$) spectrum of **Pd2a**.

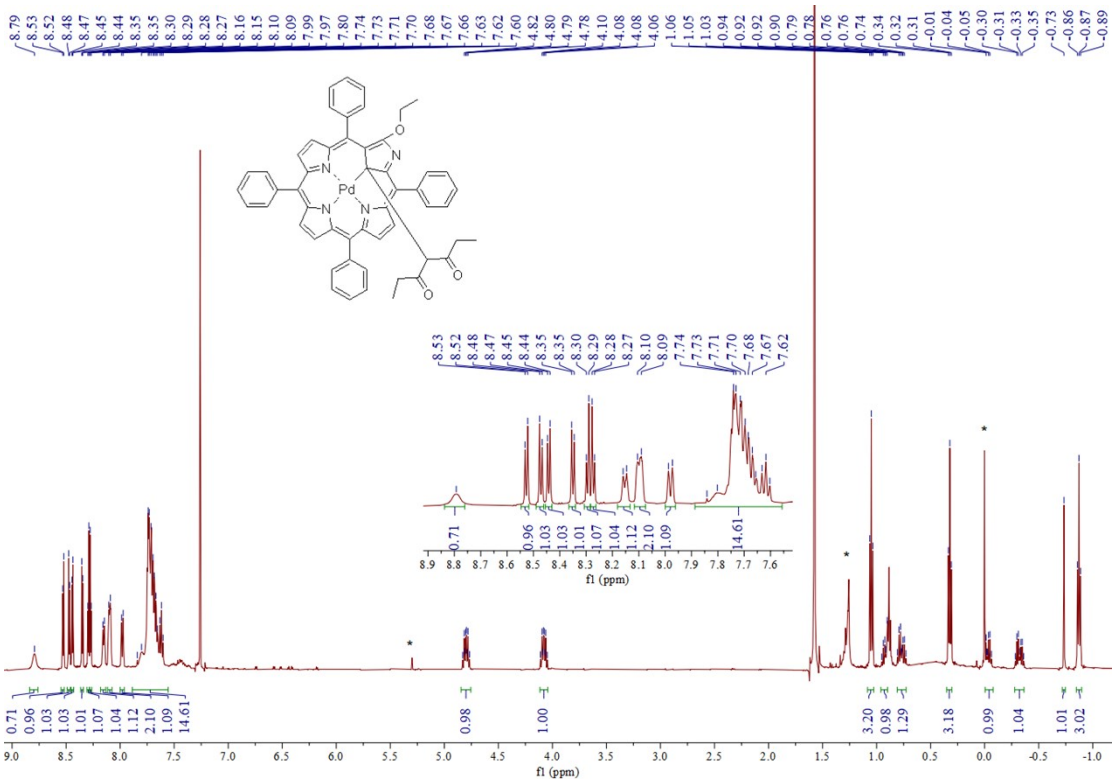

Figure S18. ^{1}H NMR (500 MHz, $CDCl_3$) spectrum of **Pd2b**. [*] solvent impurities

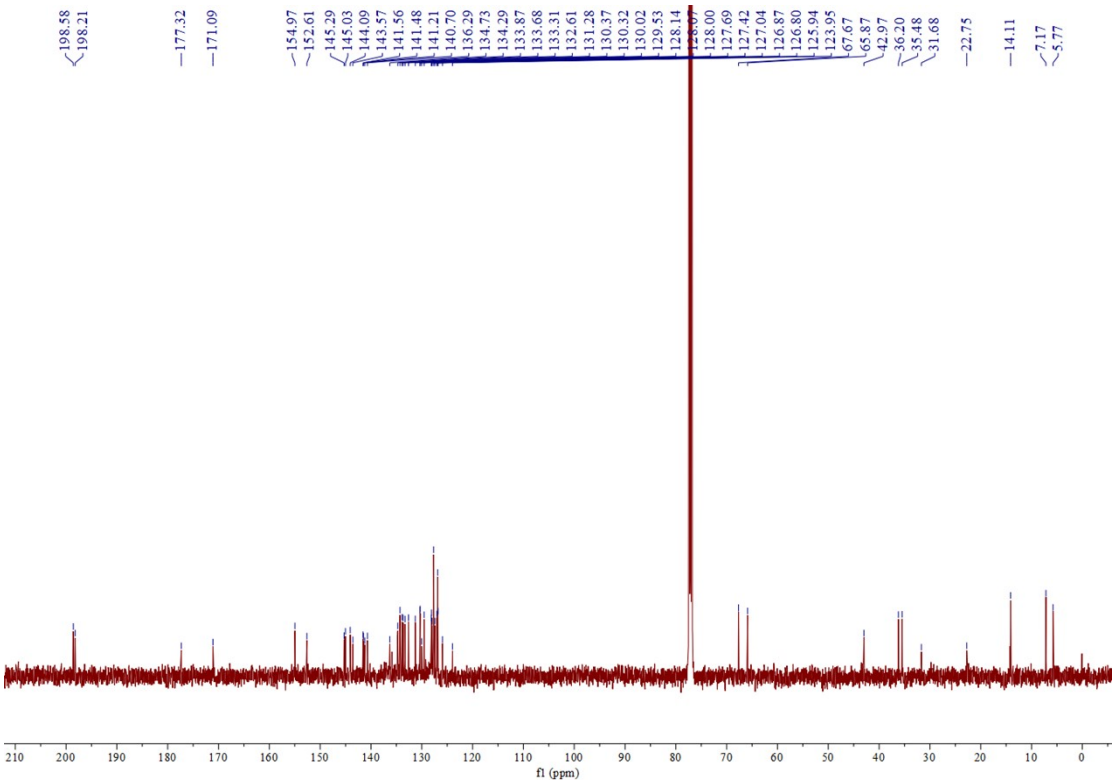

Figure S19. ^{13}C NMR (126 MHz, $CDCl_3$) spectrum of **Pd2b**.

6. Mass Spectrum

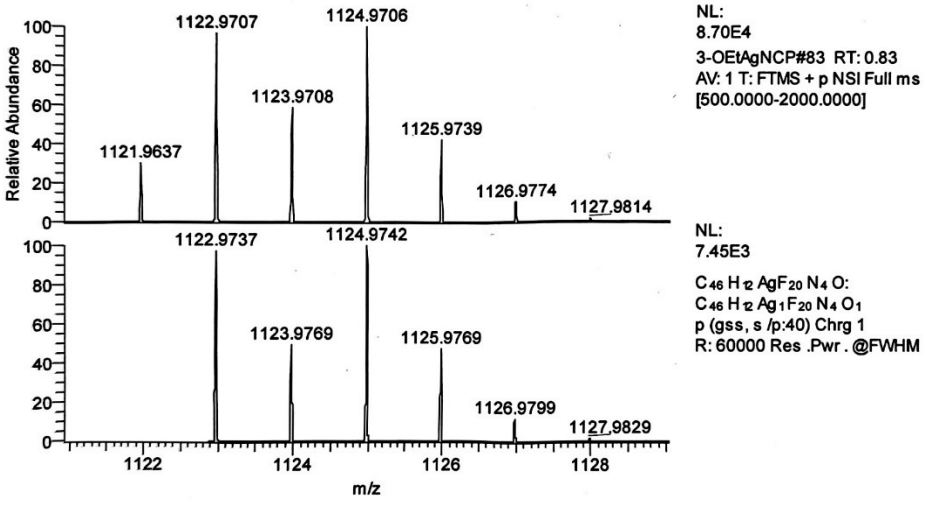

Elemental composition search on mass 1122.9707

m/z= 1117.9707-1127.9707

m/z	Theo. Mass	Delta (ppm)	RDB equiv.	Composition
1122.9707	1122.9737	-2.69	33.0	$C_{46}H_{12}ON_4AgF_{20}$

Figure S20. MALDI TOF mass spectrum of **C-3 ethoxy Ag(III) NCP**. Simulated (bottom) and observed (top).

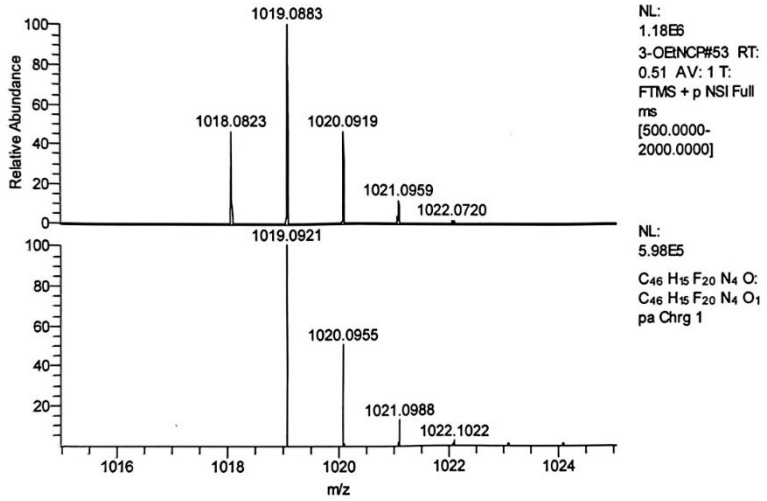

Elemental composition search on mass 1019.0883

m/z= 1014.0883-1024.0883

m/z	Theo. Mass	Delta (ppm)	RDB equiv.	Composition
1019.0883	1019.0921	-3.77	31.5	$C_{46}H_{15}ON_4F_{20}$

Figure S21. MALDI TOF mass spectrum of **C-3 ethoxy NCP**. Simulated (bottom) and observed (top).

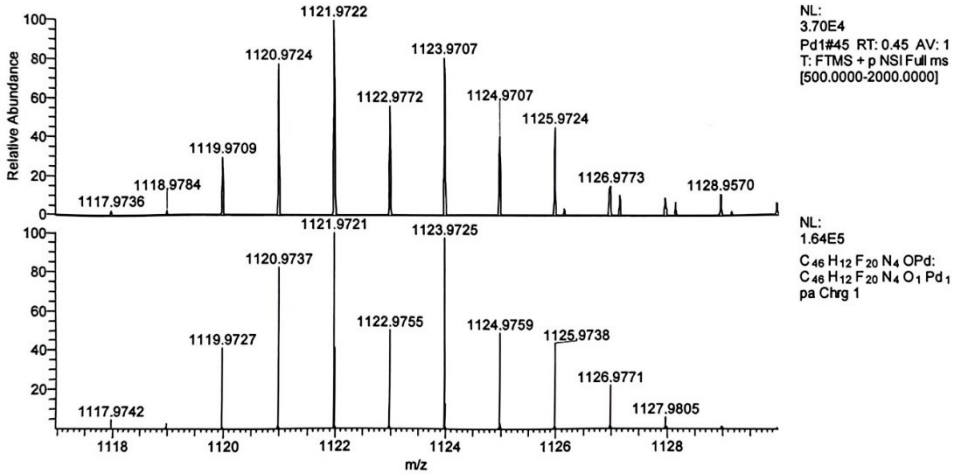

Elemental composition search on mass 1121.9722

m/z= 1116.9722-1126.9722

m/z	Theo. Mass	Delta (ppm)	RDB equiv.	Composition
1121.9722	1121.9721	0.05	33.0	$C_{46}H_{12}ON_4F_{20}Pd$

Figure S22. MALDI TOF mass spectrum of **Pd1**. Simulated (bottom) and observed (top).

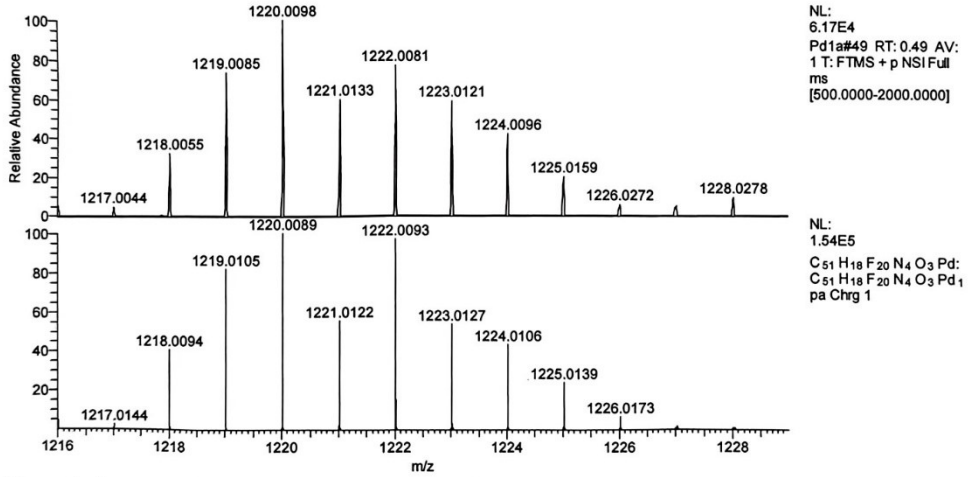

Elemental composition search on mass 1220.0098

m/z= 1215.0098-1225.0098

m/z	Theo. Mass	Delta (ppm)	RDB equiv.	Composition
1220.0098	1220.0089	0.72	35.0	$C_{51}H_{18}O_3N_4F_{20}Pd$

Figure S23. MALDI TOF mass spectrum of **Pd1a**. Simulated (bottom) and observed (top).

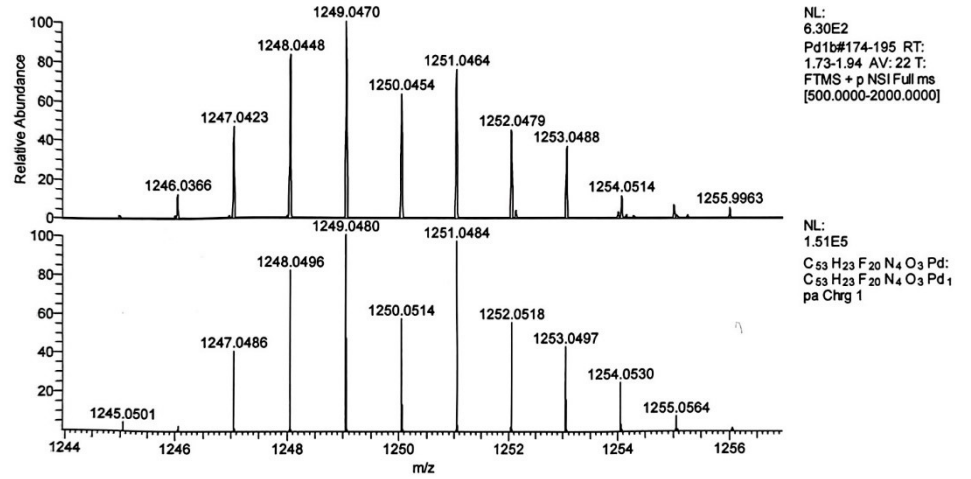

Elemental composition search on mass 1249.0470

m/z= 1244.0470-1254.0470

m/z	Theo. Mass	Delta (ppm)	RDB equiv.	Composition
1249.0470	1249.0480	-0.80	34.5	$C_{53}H_{23}O_3N_4F_{20}Pd$

Figure S24. MALDI TOF mass spectrum of **Pd1b**. Simulated (bottom) and observed (top).

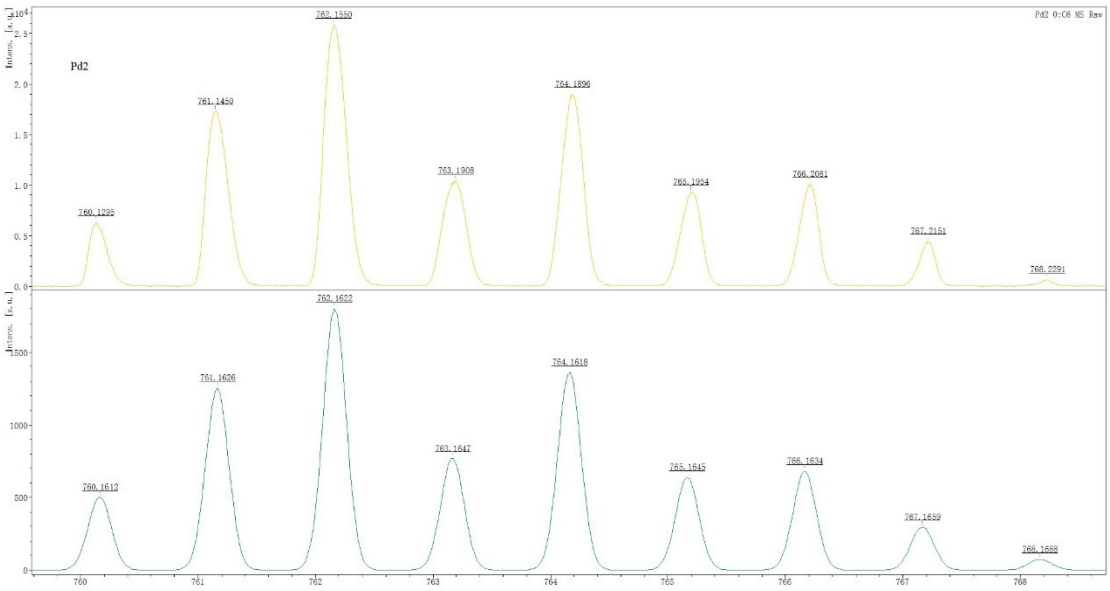

Figure S25. MALDI TOF mass spectrum of **Pd2**. Simulated (bottom) and observed (top).

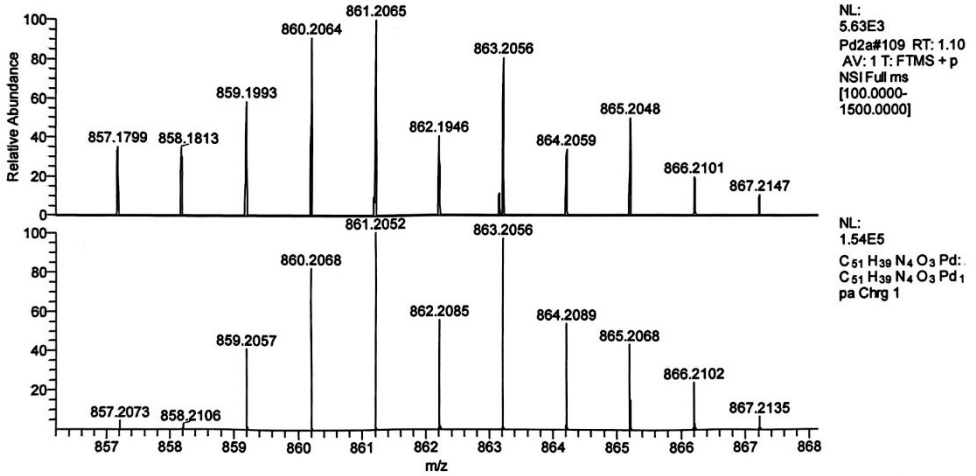

Elemental composition search on mass 861.2065

m/z= 856.2065-866.2065

m/z	Theo. Mass	Delta (ppm)	RDB equiv.	Composition
861.2065	861.2052	1.54	34.5	$C_{51}H_{39}O_3N_4Pd$

Figure S26. MALDI TOF mass spectrum of **Pd2a**. Simulated (bottom) and observed (top).

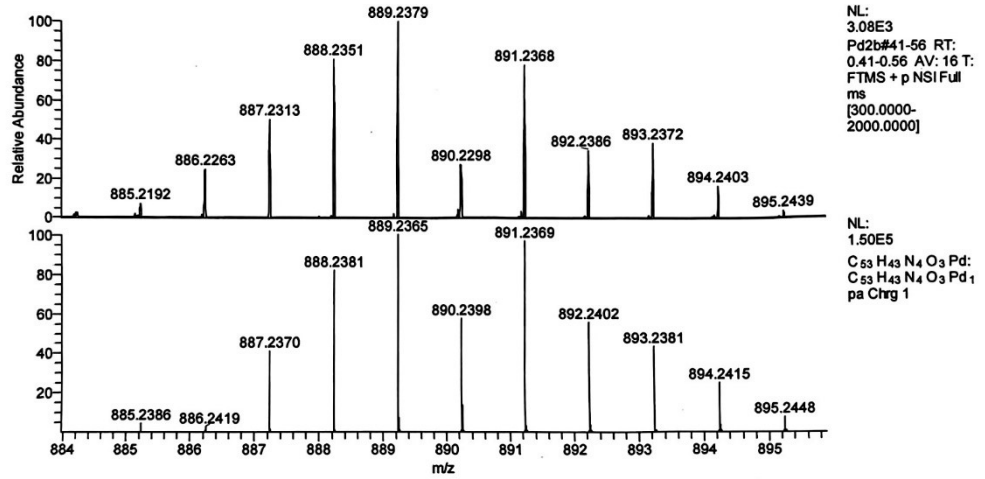

Elemental composition search on mass 889.2379

m/z= 884.2379-894.2379

m/z	Theo. Mass	Delta (ppm)	RDB equiv.	Composition
889.2379	889.2365	1.67	34.5	$C_{53}H_{43}O_3N_4Pd$

Figure S27. MALDI TOF mass spectrum of **Pd2b**. Simulated (bottom) and observed (top).

7. Electrochemical Properties

Cyclic voltammograms and differential pulse voltammograms were obtained under the following conditions: solvent: CH_2Cl_2 (Refluxed with CaH_2 under an argon atmosphere for at least 12 h and stored over 3 Å molecular sieves in a glovebox for at least 12 hours. The content of H_2O was determined by Karl Fischer titration prior to use, which was always lower than 10 ppm.), electrolyte: 0.1 M $^n Bu_4NPF_6$, working electrode: glassy carbon rod with an inner diameter of 3 mm. Working electrode was polished by 0.05 micron Al_2O_3 using the US-52 polisher (Electrical equipment Co., TaiSong). Counter electrode: Pt wire. Reference electrode: $Ag/AgNO_3$ (0.1 M $AgNO_3$ solution in CH_3CN), scan rate: 0.05 V/s. Potentials were determined vs ferrocene/ferrocenium ion by differential pulse voltammograms. Temperature: room temperature. All the measurements were taken in a glove box filled with argon.

Table S2. First and second oxidation potentials (V vs. Fc/Fc^+) of **Pd1** and **Pd2** determined by cyclic voltammetry in CH_2Cl_2.

Compounds	$E_{OX,1}$ (V)	$E_{OX,2}$ (V)
Pd1	0.355	0.787
Pd2	0.203	0.759

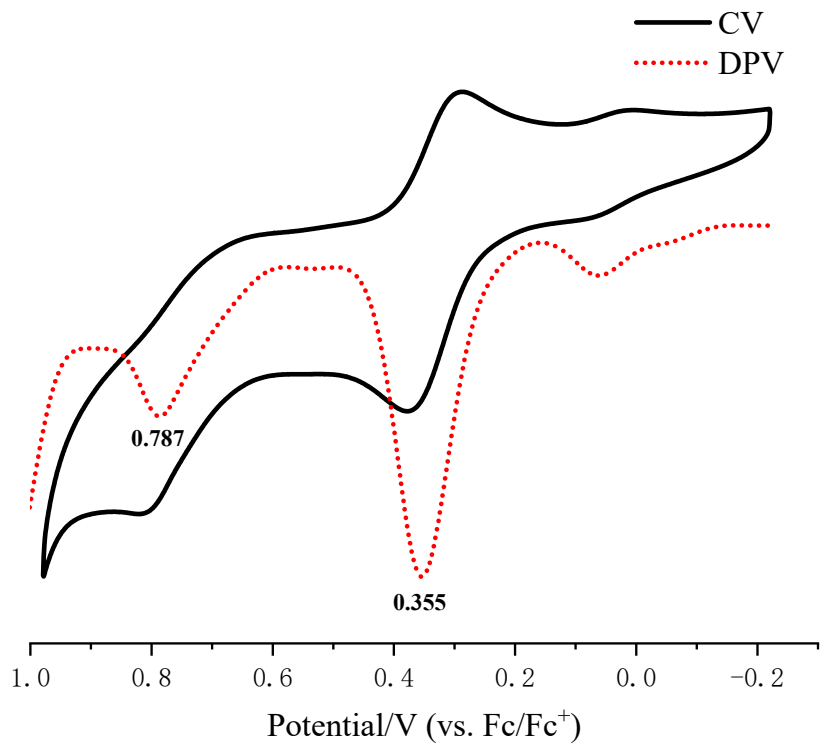

Figure S28. Cyclic voltammograms and differential pulse voltammograms of **Pd1**.

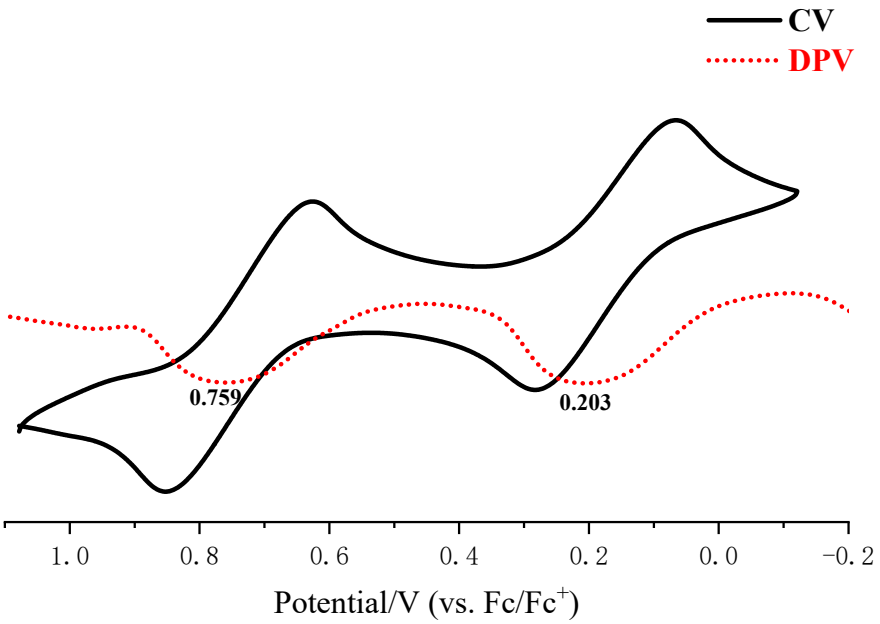

Figure S29. Cyclic voltammograms and differential pulse voltammograms of **Pd2**.

8. Resonance Hybrid of the Oxidized Intermediate

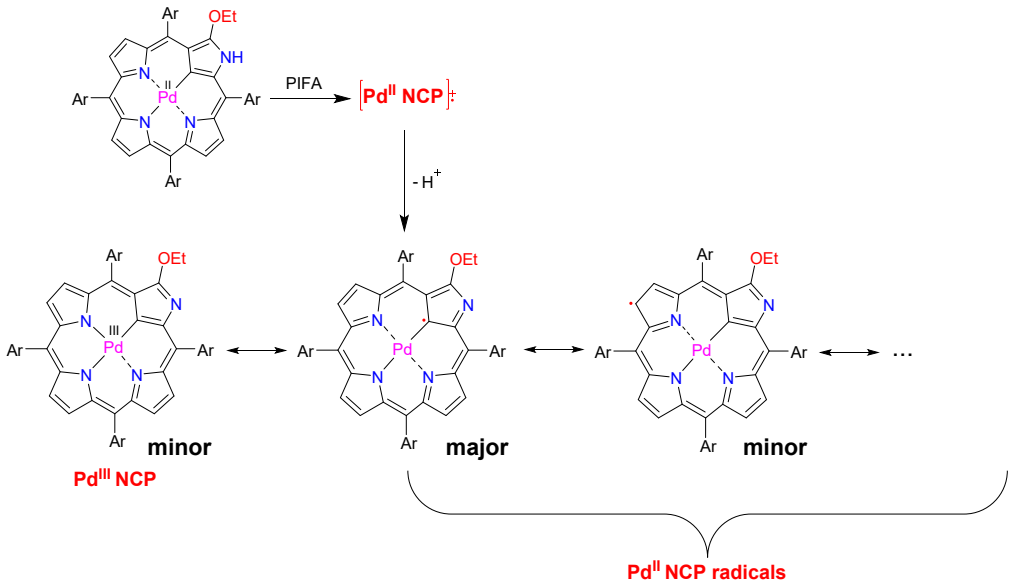

Scheme S9. Resonance hybrid of the oxidized Pd^{II} N-confused porphyrin radical.

9. Calculations

All the calculations were performed with Gaussian 16 (revision C. 01)[26]. Geometry optimizations were carried out using PBE0-D3(BJ) and a basis set of def2-SVP. Vibrational frequency analysis confirmed that the structure was either a minimum. Solvent effect (solvent = Dichloromethane) was included by single-point energy and Time-Dependent Density Functional Theory (TD-DFT calculations were performed to obtain the lowest 20 singlet excited states and elucidate the transition origins of the UV absorption spectra.) calculation using SMD model and PBE0-D3(BJ)/def2-TZVP. Wavefunction analysis, spin population, and Hirshfeld-I[27] charge analysis were performed using Multiwfn[28, 29] version 2026.3.27. Visualization of spin density and Hirshfeld-I charges was carried out using VMD. [30]

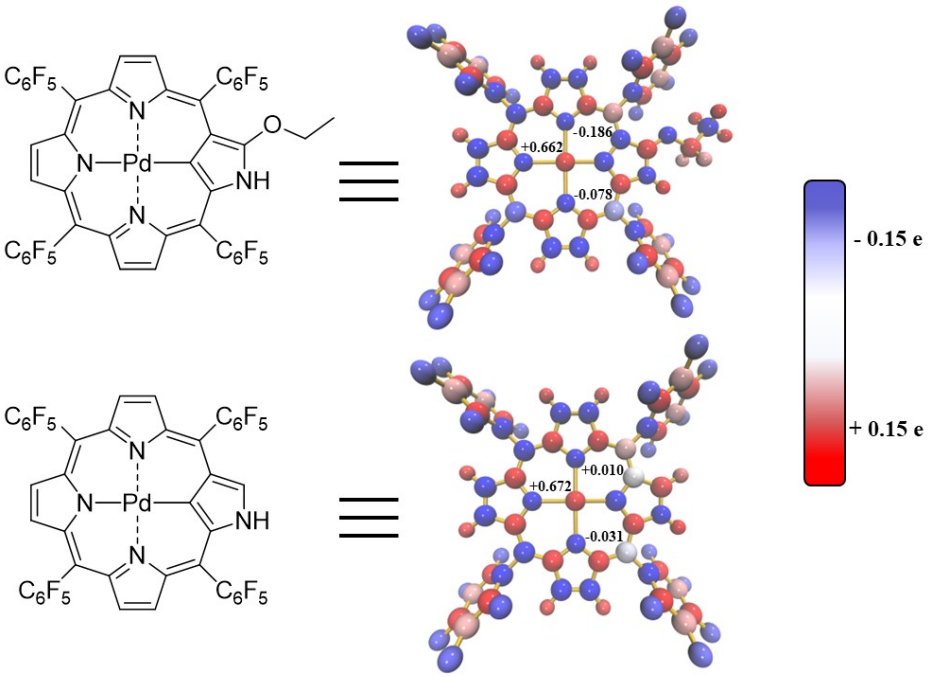

Figure S30. Hirshfeld-I charge analysis for **Pd1** and Pd NCP. Scale bar: -0.15 e to 0.15 e (blue: negative; red: positive).

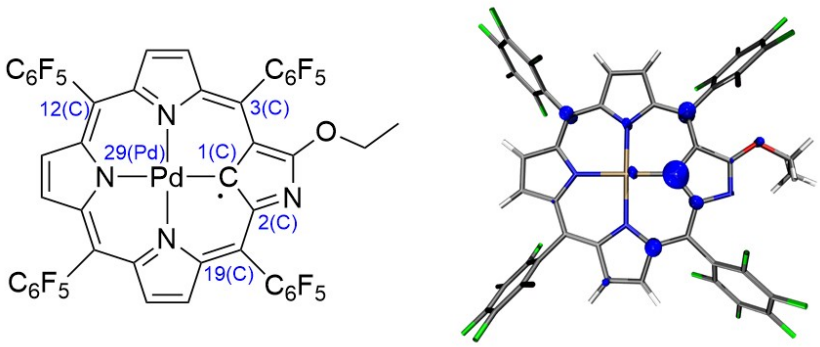

Figure S31. Spin density analysis of 3-OEt Pd NCP radical (0.015 of iso value)

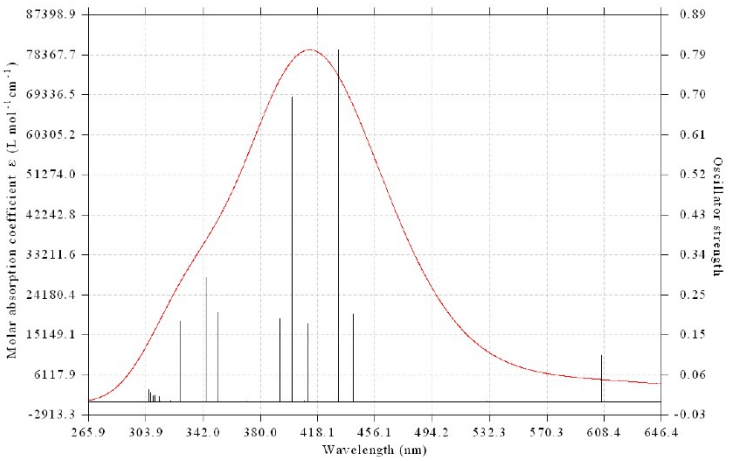

Figure S32. Simulated absorption spectrum of **Pd1**

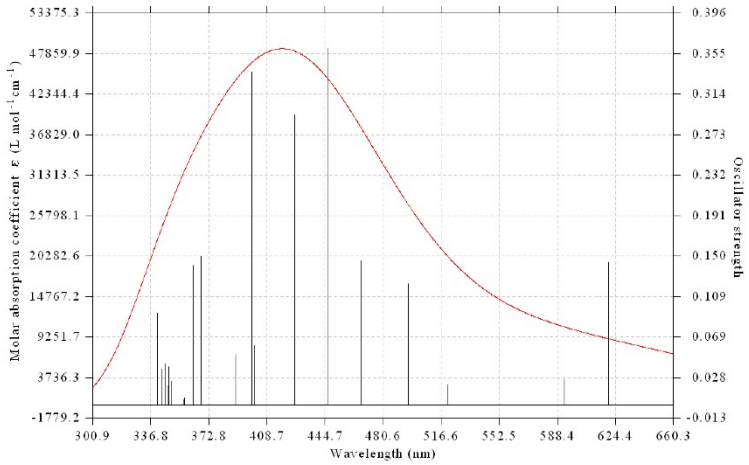

Figure S33. Simulated absorption spectrum of **Pd1a**

Hirshfeld-I charge data for Pd1 (3-OEt Pd NCP) [b]

Atom	Final atomic charges
1(C)	0.07345949
2(C)	0.24519647
3(C)	-0.1860687
4(C)	-0.20932386
5(C)	-0.23792016
6(C)	0.31724493
7(N)	-0.42615033
8(C)	-0.45849144
9(C)	0.30309117
10(N)	-0.61005898
11(C)	0.66984604
12(C)	-0.15553666
13(C)	0.3309528
14(C)	-0.23084781
15(C)	-0.21132679
16(C)	0.30577292
17(N)	-0.50101326
18(C)	-0.07775594
19(C)	0.26402671
20(N)	-0.43216137
21(C)	0.29913083
22(C)	-0.24144607
23(C)	-0.22355696
24(C)	-0.12194355
25(C)	-0.29650742
26(C)	-0.25462904
27(C)	-0.22404555
28(C)	-0.23480206
29(Pd)	0.66201558

30(C)	0.26237778
31(C)	0.06584195
32(C)	0.14589566
33(C)	0.06418981
34(C)	0.26081818
35(C)	0.25086765
36(C)	0.06714345
37(C)	0.14485102
38(C)	0.06400919
39(C)	0.23609139
40(C)	0.24702625
41(C)	0.06465188
42(C)	0.1425086
43(C)	0.06458297
44(C)	0.24690502
45(C)	0.24871003
46(C)	0.06413224
47(C)	0.1428811
48(C)	0.06435414
49(C)	0.24977086
50(F)	-0.11557911
51(F)	-0.11250538
52(F)	-0.11177643
53(F)	-0.12259699
54(F)	-0.11992504
55(F)	-0.10921278
56(F)	-0.11023157
57(F)	-0.1069266
58(F)	-0.11504898
59(F)	-0.12274906
60(F)	-0.11239847
61(F)	-0.11508177
62(F)	-0.11254926
63(F)	-0.12313974
64(F)	-0.12241786
65(F)	-0.11254391
66(F)	-0.11498366
67(F)	-0.11239637
68(F)	-0.12251241
69(F)	-0.12863632
70(O)	-0.2753404
71(C)	0.13905819
72(C)	-0.53579755
73(H)	0.12739895
74(H)	0.1308717
75(H)	0.35489831
76(H)	0.13079654
77(H)	0.12919411

78(H)	0.1298289
79(H)	0.12483166
80(H)	0.07296771
81(H)	0.07755344
82(H)	0.16793813
83(H)	0.1546564
84(H)	0.15959544

Hirshfeld-I charge data for Pd NCP [b]

Atom	Final atomic charges
1(C)	0.05524615
2(C)	0.23521096
3(C)	0.0099005
4(C)	-0.19530891
5(C)	-0.24303843
6(C)	0.33291817
7(N)	-0.42290685
8(C)	-0.50998689
9(C)	0.25945401
10(N)	-0.39687818
11(C)	0.13789058
12(C)	-0.16783084
13(C)	0.34382082
14(C)	-0.22413463
15(C)	-0.20997027
16(C)	0.32645042
17(N)	-0.51445512
18(C)	-0.03089513
19(C)	0.25166531
20(N)	-0.42831821
21(C)	0.32053177
22(C)	-0.24476825
23(C)	-0.2077894
24(C)	-0.14653016
25(C)	-0.30220409
26(C)	-0.2809756
27(C)	-0.22619488
28(C)	-0.23279028
29(Pd)	0.67158749
30(C)	0.25203054
31(C)	0.0657827
32(C)	0.14481289
33(C)	0.06632903
34(C)	0.25771048
35(C)	0.2558547
36(C)	0.06700908
37(C)	0.14625394
38(C)	0.06629306

39(C)	0.23985348
40(C)	0.24662914
41(C)	0.06441455
42(C)	0.14257483
43(C)	0.06471643
44(C)	0.24626229
45(C)	0.24729862
46(C)	0.06419535
47(C)	0.14272242
48(C)	0.06435621
49(C)	0.24825969
50(F)	-0.11075607
51(F)	-0.10895397
52(F)	-0.10819534
53(F)	-0.11943489
54(F)	-0.11906011
55(F)	-0.10656057
56(F)	-0.1083043
57(F)	-0.10534852
58(F)	-0.1148052
59(F)	-0.11976928
60(F)	-0.11032207
61(F)	-0.11301613
62(F)	-0.11050234
63(F)	-0.12083971
64(F)	-0.11976803
65(F)	-0.11036125
66(F)	-0.11286525
67(F)	-0.11028065
68(F)	-0.12042008
69(F)	-0.12443783
70(H)	0.12960044
71(H)	0.13295454
72(H)	0.33749031
73(H)	0.13262828
74(H)	0.1315069
75(H)	0.13204783
76(H)	0.12811002
77(H)	0.09660375

Spin population analysis of the one-electron-oxidized 3-ethoxy Pd^{II} N-confused porphyrin radical. [b]

Atom	Spin pop.
1(C)	0.38513
2(C)	0.10795
3(C)	0.18835
4(C)	-0.06378
5(C)	-0.11715

6(C)	0.00023
7(C)	-0.00722
8(C)	-0.0562
9(N)	0.06776
10(N)	0.03001
11(C)	0.07061
12(C)	0.15101
13(C)	-0.05345
14(C)	0.0774
15(C)	-0.05304
16(C)	0.07126
17(N)	0.00215
18(C)	-0.09314
19(C)	0.179
20(N)	-0.056
21(C)	0.06742
22(C)	0.08703
23(C)	-0.03785
24(C)	-0.00791
25(C)	-0.01614
26(C)	0.00101
27(C)	-0.00972
28(C)	-0.00157
29(Pd)	0.13765
30(C)	0.00901
31(C)	-0.00361
32(C)	0.00646
33(C)	-0.00327
34(C)	0.00847
35(C)	-0.00257
36(C)	0.00167
37(C)	-0.00266
38(C)	0.00172
39(C)	-0.00323
40(C)	0.00656
41(C)	-0.00191
42(C)	0.00385
43(C)	-0.00213
44(C)	0.00476
45(C)	-0.00122
46(C)	0.00009
47(C)	0.00003
48(C)	0.00044
49(C)	0.00118
50(F)	0.00057
51(F)	-0.00011
52(F)	-0.00009
53(F)	0.00026

54(F)	-0.00002
55(F)	0.00006
56(F)	-0.00023
57(F)	0.00007
58(F)	0.00014
59(F)	0.00025
60(F)	0.00005
61(F)	0.00001
62(F)	0.00001
63(F)	-0.00003
64(F)	0.00004
65(F)	-0.00005
66(F)	0.00035
67(F)	-0.00003
68(F)	0.0002
69(F)	0.00023
70(O)	0.03019
71(C)	-0.00291
72(C)	0.00222
73(H)	0.00066
74(H)	0.00109
75(H)	-0.00348
76(H)	0.00253
77(H)	-0.00514
78(H)	0.00075
79(H)	0.00043
80(H)	0.00163
81(H)	-0.00013
82(H)	-0.00016
83(H)	-0.00003

b Atom numbering follows the computational output and may differ from the labeling used in the main text.